Observing middle and inner ear mechanics with novel intracochlear pressure sensors

Elizabeth S. Olson[a)]
Physics Department, Princeton University, Princeton, New Jersey 08544

(Received 16 July 1997; revised 17 February 1998; accepted 18 February 1998)

Intracochlear pressure was measured *in vivo* in the base of the gerbil cochlea. The measurements were made over a wide range of frequencies simultaneously in scalae vestibuli and tympani. Pressure was measured just adjacent to the stapes in scala vestibuli and at a number of positions spaced by tens of micrometers, including a position within several micrometers of the basilar membrane, in scala tympani. Two findings emerged from the basic results. First, the spatial variation in scala tympani pressure indicated that the pressure is composed of two modes, which can be identified with fast and slow waves. Second, at frequencies between 2 and 46 kHz (the upper frequency limit of the measurements) the scala vestibuli pressure adjacent to the stapes had a gain of approximately 30 dB with respect to the pressure in the ear canal, and a phase which decreased linearly with frequency. Thus, over these frequencies the middle ear and its termination in the cochlea operate as a frequency independent transmission line. A subset of the data was analyzed further to derive the velocity of the basilar membrane, the pressure difference across the organ of Corti complex (defined to include the tectorial and basilar membranes) and the specific acoustic impedance of the organ of Corti complex. The impedance was found to be tuned in frequency. © *1998 Acoustical Society of America.* [S0001-4966(98)00906-0]

PACS numbers: 43.64.Kc, 43.64.Ha, 43.64.Yp, 43.38.Kb [RDF]

INTRODUCTION

The cochlea is a fluid dynamic system. Of special interest is the motion of the cochlea's organ of Corti (O.C.) because it stimulates hair cells, and this motion has been the emphasis of intracochlear experimentation and models of cochlear mechanics. One force driving the motion is the fluid pressure difference across the organ of Corti. Localized measurements of pressure, and the pressure gradients that indicate fluid motion, are key to understanding the motion and mechanics of the organ of Corti, and cochlear fluid dynamics in general. On another note, scala vestibuli (S.V.) pressure near the stapes, the ''input'' pressure to the inner ear, is also the ''output'' of the middle ear, and its measurement is key to understanding the middle ear's operation.

In previous studies the pressure measured near the stapes in S.V. has been used to estimate the cochlear input impedance and to determine the gain of the middle ear (Dancer and Franke, 1980; Nedzelnitsky, 1980; Lynch *et al.*, 1982; Decory *et al.*, 1990). The current measurements extend those measurements to another species and include much higher frequencies. The frequency range extended from either 200 or 500 Hz to 46 kHz, which comprises much of the approximately 60-kHz auditory range of the gerbil (Ryan, 1976). A particularly simple relationship between the S.V. pressure just inside the stapes and the pressure in the ear canal emerged at frequencies between 2 and 46 kHz. The pressure gain was relatively flat, at approximately 30 dB, and the linear phase versus frequency relationship could be characterized as a constant 25-μs delay. The gain decreased as the frequency was reduced below 2 kHz, and was approximately 10 dB at 200 Hz.

Intracochlear pressure is fundamentally a field, and for illuminating cochlear mechanics examining the pressure's spatial variation is essential. In the current study the pressure field in scala tympani (S.T.) was mapped close to the basilar membrane (B.M.) through the round window opening. The S.T. pressures and spatial variations that were found can be economically interpreted as being a combination of two pressure modes, a ''fast wave'' mode and a ''slow wave'' mode. The fast mode was dominant at positions relatively far from the B.M. and the slow mode at positions less than 100 μm from the B.M. The fast and slow waves have been discussed in the theoretical and experimental literature. In a theoretical model Peterson and Bogart (1950) showed that the pressure in the cochlea could be mathematically separated into a component that traveled with the speed of sound (fast) and a component that traveled at the speed of the O.C. traveling wave (slow). Because it is linked to the O.C. traveling wave, the slow mode has been emphasized in most cochlear models. However, Lighthill (1981) suggested that the fast wave might be responsible for the high frequency plateaus in B.M. motion found by Rhode (1971) and subsequently in many other B.M. motion studies (Ruggero *et al.*, 1997; Nuttall and Dolan, 1996; Ulfendahl and Khanna, 1993; Cooper and Rhode, 1992a). The fast wave was implicated by Cooper and Rhode (1996) in producing artifactual O.C. motions in cochleae in an unnatural condition (open apex). Dancer and Franke (1980) discussed the two pressure waves, and the associated difficulty of using point intracochlear pressure measurements to find the pressure across the O.C. complex.

The spatial variation of the S.T. pressure and in particular the emergence of a slow wave pressure close to the B.M.

a)Electronic mail: olson@pupgg.princeton.edu

Downloaded 30 Jun 2010 to 156.145.57.60. Redistribution subject to ASA license or copyright; see http://asadl.org/journals/doc/ASALIB-home/info/terms.jsp

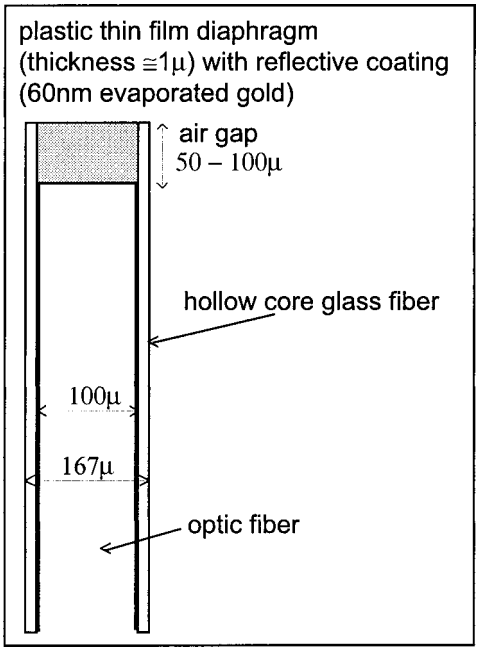

FIG. 1. Fiber optic pressure sensor tip. During measurements the pressure sensitive diaphragm was located at the measurement position within the cochlea or ear canal. The optic fiber that is shown threaded into the sensor tip is one of two output arms of a fiber coupler. The second output arm is not used. The two input arms are coupled to a LED, which delivers light to the sensor diaphragm, and a photodiode, which detects the light that reflects off the diaphragm.

underscore the intimate link between the intracochlear pressure field and the motion of the O.C. complex. The final analysis demonstrates the use of the pressure data to estimate the quantitative form of the impedance of the O.C. complex, and finds that it is tuned.

It is important to note at the outset that the condition of the cochleae, as determined from changes in compound action potential threshold, was not optimal.

I. METHODS

A. Sensor

The sensor is illustrated in Fig. 1. The sensor has been described briefly (Olson and Borawala, 1997), and its construction is detailed here.

1. Sensor tip

The sensor tip is composed of a hollow core glass fiber (inner diameter 100 μm, outer diameter 167 μm, Polymicro Technologies, Phoeniz, AZ), terminated with a pressure sensitive diaphragm made reflective with a thin layer of gold. The diaphragm is a plastic thin film, formed by floating a drop of photosensitive polymer adhesive (Norland, New Brunswick, NJ, type #68) on water. With proper surface tension, vessel and drop size, the drop expands into a thin film of submicron thickness (Zhou *et al.*, 1993). The thickness is estimated by the interference-induced coloration of the film, in a manner described in texts on electron microscopy. As the adhesive expands bands of bright interference colors become visible, and then fairly broad regions of one color. At that point, the film is probably less than one optical wavelength in thickness, some hundreds of nanometers. The floating adhesive is cured with ultraviolet light for 5 min. Following curing the film appears thicker, but bright interference colors are still present, indicating that the thickness is still on the order of a micrometer. (Films several micrometers thick appear clear, not colored.) The diaphragm is formed by scooping up the floating film with a glass hollow core fiber. The sensor tip is cured for at least 15 additional minutes. The hollow core fiber is prepared by removing sections of the outer plastic coating using the heat of a microelectrode puller and cleaving the fiber into sections 1–2 cm in length, with blunt perpendicular ends. After a batch of diaphragms was prepared, 50–60 nm of gold was evaporated on their outer surfaces to make them reflective.

2. Optical system

The position of the diaphragm is read optically, using an optic lever. Optic levers are available commercially (Optoacoustic sensors, Raleigh, NC), although the one in use is home-made. Much larger optic-lever-based microphones have been described previously (Hu *et al.*, 1992). The LED light is delivered down one of the input fibers of an optic fiber coupler with a 50:50 splitting ratio (Gould Corp., Millersville, MD). The light that returns in the second input arm is collected by a photodiode. Only one output fiber is used (the other is optically sunk), and it is etched down from its original 125 μm diameter to slightly less than 100 μm by soaking in 6% hydrofluoric acid for 4 h. After etching, the output fiber is cleaved to a blunt 90 degree angle, which is monitored both under the microscope, and by the amount of light reflected off the blunt surface.

The output fiber is threaded into the sensor tip and glued in position (using Norland adhesive NEA 123) with the fiber end 50 to 100 μm from the diaphragm. In operation, the LED light fans out as it exits the fiber, reflects from the diaphragm, and returns to the fiber. The amount of light that reenters the fiber core for transmission back to the photodiode depends on the distance to the diaphragm. This position detection scheme, based on geometric optics, is the essence of an optic lever. In order to control the quality of the constructed sensors, in practice the fiber is threaded into different tips until a high level of reflected light is collected by the fiber. Prior to fixing the fiber in place, the response to acoustic stimuli is checked in air. The sensors are fragile, and might be used in many experiments, or be broken almost immediately. The fiber couplers can be reused. At least three sensors are on hand during an experiment. Complete sensors are made up at least a few days prior to an experiment so that their sensitivity and stability can be checked. Sensors have lasted up to 8 months.

The linear working range of an optic lever depends on the fiber size and is roughly equal to the fiber radius, at a position approximately one fiber diameter from the reflector. In operation in the pressure sensor the fiber–reflector distance is modulated by the diaphragm's pressure induced deflections, and the variation in returning light comprises the sensor's output signal. Based on the sensor stiffness (see below) the deflections we expect are at the most tens of nanometers, well within the working range.

Downloaded 30 Jun 2010 to 156.145.57.60. Redistribution subject to ASA license or copyright; see http://asadl.org/journals/doc/ASALIB-home/info/terms.jsp

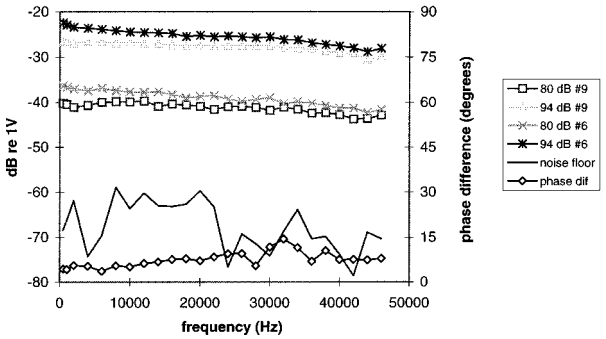

FIG. 2. Absolute sensor calibration in fluid. A vibrating fluid column was used to deliver a known pressure to the sensor over a wide range of frequencies. The stimulus level in dB SPL is indicated in the legend. The sensor responses are almost flat with frequency, and the calibrations are represented by a single value at all frequencies. Sensor #6 would be calibrated at −38 dBV/80 dB SPL, sensor #9 at −41 dBV/80 dB SPL. The noise level shown corresponds to roughly 60 dB SPL and was determined in the absence of stimulation with 6.4 s of signal averaging. During experiments signals were typically averaged for 3.2 s, and the noise floor was approximately 65 dB SPL. The phase differences between sensor #6 and its electronic system and sensor #9 and its electronic system are less than 15°. When analyzing experimental data, phase data taken with one sensor at one location (S.T. or S.V.) are referenced to phase data taken with another sensor in another location (S.V. or ear canal).

3. Sensor calibration

a. In fluid. The sensitivity, as photodetector voltage/pressure, was calibrated by delivering a known pressure to the sensor by immersing it in a vibrating column of water (Schloss and Strassberg, 1962; Nedzelnitsky, 1980). The sensor head was immersed a prescribed distance (typically 0.5 to 2 mm) under the surface of a small vial of water on a dynamic shaker with a built-in monitor accelerometer (Bruel & Kjær model 4290). The shaker was vibrated at a prescribed acceleration over 25 frequencies ranging between 0.5 and 46 kHz. The shaker produces a hydrodynamic pressure proportional to the immersion depth, the fluid density, and the acceleration amplitude. At high frequencies the effects of the acoustic standing wave set up in the vial modify the simple proportionality, and the depth of the fluid column must be accounted for (Schloss and Strassberg, 1962). Due to the small vial size, the standing wave correction is small even at the highest frequencies (less than 20%). Nevertheless, the correction is made in the calibration. In Fig. 2, the shaker amplitude was set to deliver calibration pressures of 80 and 94 dB SPL. The responses of two sensor/electronic systems are shown. The calibrations are nearly flat with frequency, indicating that the diaphragm's motion in response to pressure is dominated by the sensor/diaphragm stiffness. (See more on the sensor impedance below.) Both sensors show a slow decrease that accumulates 3 (#9) or 6 dB (#6) over the 46-kHz span, suggesting that viscous drag is not completely negligible. With 6.4 s of signal averaging the signal of 80 dB SPL is 20 dB out of the noise. Sensor linearity has been verified at levels ranging from 70 to 120 dB SPL. Figure 2 shows that the two sensor/electronic systems have nearly equal phases. This was generally true, and is essential because all of the pressure data is referenced to pressure data taken with a similar sensor.

A measure of the absolute phase of the sensor was made by referencing it to the phase of the shaker's monitor accelerometer. The pressure induced by the shaker's motion in theory is in phase with the acceleration of the shaker. If the sensor's specific acoustic impedance is dominated by acoustic stiffness, the phase of the sensor output will be in phase with pressure, and thus will be in phase with the output of the monitor accelerometer. The phase difference between the sensor and the accelerometer was found to be close to zero at the lowest frequencies, and to decrease monotonically to −30 degrees at 46 kHz. The phase departure from zero might indicate that, in deflecting the sensor diaphragm, the pressure is working not just against the stiffness of the diaphragm and air gap, but against viscosity in the fluid or diaphragm. This explanation is consistent with the small decrease in the magnitude of the sensitivity as frequency is increased.

The small decrease in the magnitude of the sensitivity with frequency was not accounted for because it is similar in size to inherent calibration uncertainties. The calibrated sensitivity of a sensor sometimes changed during the course of an experiment, introducing an uncertainty in the calibration of up to ± 6 dB. When calibration changes occurred, they included all frequencies approximately equally. Changes $\geqslant 4$ dB occurred in at least one sensor in 50% of the experiments. In order to minimize this uncertainty, sensors were recalibrated whenever it was practical in the course of an experiment. (See Sec. I E below.)

b. In air. Independent calibrations were performed using the substitution method, in air. Tones were measured with a Bruel & Kjær microphone ($\frac{1}{4}$ in. model 4135), and then with a sensor placed in the same sound field. The relative outputs of the sensor and the microphone, and the factory specified sensitivity of the microphone were used to calibrate the sensor. Sensor calibrations in air were flat with frequency, with a value within a few dB of the sensitivity in water. The phase of the sensor output relative to the microphone was close to zero at the lowest frequencies, and 10 to 20 degrees at frequencies above 40 kHz. The maximum variation, 35 degrees, occurred between 20 and 30 kHz, where the microphone sensitivity exhibits small dips and peaks. At these frequencies, it is likely that the phase difference occurs because the impedance of the microphone is not simply that of an acoustic stiffness.

4. Sensor impedance: The ratio of pressure to diaphragm velocity

The specific acoustic (S.A.) impedance of the sensor, defined as the ratio of sound pressure to the velocity of a center point on the diaphragm, is critical to gauging whether, and to what degree, the sensor loads the measurement. The sensor's S.A. impedance is expected to be dominated by S.A. stiffness, and the calibration described above supports this expectation. The S.A. stiffness has two additive components: the diaphragm's S.A. stiffness, and the S.A. stiffness of the air gap between the diaphragm and the fiber end. The Young's modulus of the diaphragm material is reported by the manufacturer as 0.14 GPa, and plate theory predicts a

Downloaded 30 Jun 2010 to 156.145.57.60. Redistribution subject to ASA license or copyright; see http://asadl.org/journals/doc/ASALIB-home/info/terms.jsp

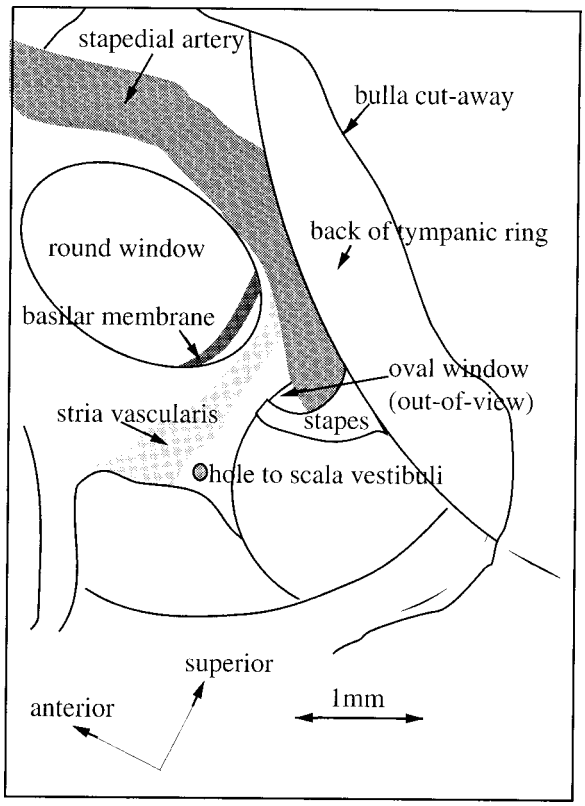

FIG. 3. The approach to the cochlea. The drawing is traced from a photomicrograph. The S.V. sensor was inserted into the hole indicated, usually to a depth between 0.25 and 1 mm. The S.T. sensor was inserted via the round window opening following removal of the round window membrane. The CAP electrode was positioned on the bone outside the round window opening.

S.A. stiffness (pressure/center deflection) slightly greater than 0.1 Pa/nm for a circular plate of 1-μm thickness and 100 μm diameter (Timoshenko and Woinowsky-Krieger, 1959). The S.A. stiffness is proportional to diaphragm thickness cubed, so small variations in thickness produce relatively large variations in stiffness. Tension in the plate will increase the stiffness, but because the adhesive is cured before being attached to the hollow core fiber, it is not expected to be under tension. The S.A. stiffness of a 100-μm-deep air gap (air gap depths vary between 50 and 100 μm) is calculated as either approximately 1 Pa/nm (isothermal compression, where PV = constant) or 1.4 Pa/nm (adiabatic compression, where PV^{γ}= constant, and γ, the specific heat ratio, has a value of 7/5 in air). Air gap stiffness scales as 1/gap depth, so a 50-μm gap has twice this stiffness. In summary, the air gap stiffness should dominate and the total S.A. stiffness should have a value of approximately 2 Pa/nm. This is best considered a lower bound due to uncertainty in the diaphragm stiffness.

The sensor S.A. stiffness should be compared with the S.A. stiffness of the organ of Corti. *In vivo* measurements of O.C. stiffness at the same longitudinal position as the current measurements found a mechanical stiffness of approximately 7 N/m [20-μm-diameter probe tip, radially centered measurements (Olson and Mountain, 1994)]. With a beam model of the O.C. this translates to a S.A. stiffness of approximately 4 Pa/nm (Olson and Mountain, 1991). Therefore, the sensor has a S.A. stiffness similar to that of the O.C. complex, and when it is close to the basilar membrane it is likely to reduce the pressure.

The sensor's acoustic impedance (pressure/volume velocity) should also be compared with the cochlear input acoustic impedance, which is primarily resistive, with a value of approximately 10^{11} Pa m^{-3}s in cat (Lynch *et al.*, 1982). (No data on gerbil are available.) The acoustic impedance of the sensor is proportional to 1/frequency, and at 40 kHz is calculated as 10^{12} Pa m^{-3}s. Therefore, the sensor's acoustic impedance is substantially larger than that of the cat cochlea even at the highest frequencies. If the gerbil cochlea is similar, the sensor is not expected to reduce the cochlear input pressure substantially.

5. Spatial resolution of the sensor

In order to resolve cochlear micromechanics, the sensor diameter should be at most half the size of the traveling wave wavelength. The wavelength varies both with frequency and with longitudinal location. At a given longitudinal location, it is expected to be smallest at the local characteristic frequency (c.f.) (Lighthill, 1981). Rhode (1971) found the c.f. wavelength to be 1.5 mm at the 7-kHz place in squirrel monkey. Cooper and Rhode (1992a) found the c.f. wavelength to be 0.6 mm in cat and 0.9 mm in guinea pig, in both cases at the 31-kHz place. Three-dimensional passive cochlear models indicate a wavelength of approximately 1 mm (Steele, 1974, 1-kHz place). Therefore, it is reasonable to believe that the sensor's 0.1-mm-diameter diaphragm is capable of resolving cochlear micromechanics.

B. Animal

1. Basic preparation

The experimental animals were young adult mongolian gerbils (*Meriones unguiculatus*) 40 to 60 g in weight. The gerbil was given a subdermal injection of the analgesic tranquilizer acepromazine (dose 1 mg/kg) followed by an intraperitoneal injection of the anesthetic sodium pentobarbital (initial dose 60 mg/kg). Supplemental 10 mg/kg doses of sodium pentobarbital were given when deemed necessary from a toe pinch response. The animal temperature was maintained at 38 °C with an animal blanket and a room heater. To maintain a clear airway, a slit was made in the trachea. The anesthetized animal was secured in a stereotaxic frame on its back and surgery was performed to expose the left cochlea. The pinna was removed and an earphone tube was positioned into the ear canal. The bulla was widely opened, as indicated in Fig. 3, during all data collection. A silver wire electrode, insulated to its tip, was placed on the bone just outside the round window opening. With it, the compound action potential (CAP) response to tone pips was measured as a monitor of cochlear condition. At or close to the end of an experiment animals were euthanized with an overdose of anesthetic.

Downloaded 30 Jun 2010 to 156.145.57.60. Redistribution subject to ASA license or copyright; see http://asadl.org/journals/doc/ASALIB-home/info/terms.jsp

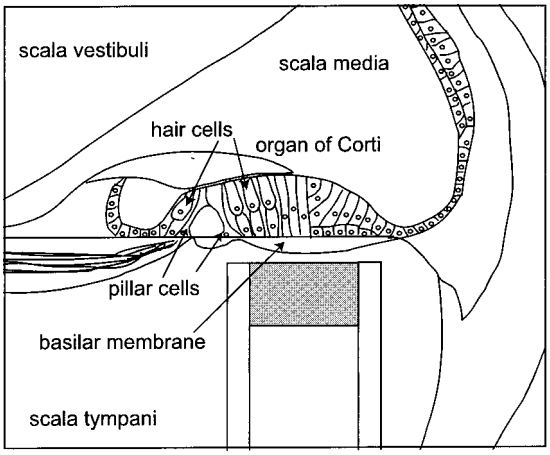

FIG. 4. Position of the S.T. sensor. This sketch shows an ideal approach to the basilar membrane: the sensor is centered radially, and approaches perpendicularly. The outer diameter of the sensor is 167 μm, and is drawn approximately to scale. The drawing of the O.C. derives from a 2 μm plastic-embedded section prepared by Dr. Martin Feldman of Boston University School of Medicine.

2. Sensor approach for intracochlear pressure measurements

Figure 3 illustrates the approach. In order to access scala vestibuli, a hole just large enough to accommodate a sensor was hand drilled through the cochlear bone adjacent to the oval window, in the region between the oval and round windows. The S.V. sensor was held in a micromanipulator attached to the stereotaxic frame. The sensor was inserted less than 1 mm into the hole unless otherwise noted. It was not sealed into the cochlea with cement or glue, but was mechanically quite well sealed in most experiments because of the precise hole size.

Scala tympani was accessed through the round window opening following removal of the round window membrane. Part of the basal turn of the basilar membrane is visible through the round window, and the S.T. sensor was angled to approach the B.M. perpendicularly, and (typically) centered radially, as indicated in Fig. 4. The c.f. at this position is close to 30 kHz (Xue *et al.*, 1995). Perilymph often wells out of the round window opening after removing the membrane. In order to control the perilymph fluid level, in later experiments a wick was positioned behind the round window opening. Sensor fibers were held in a glass micropipette glued to a stainless steel rod, with less than 2 cm emerging. A small amount of modeling clay fixed the sensor fiber where it emerged from the pipette, so that it could not move laterally within the pipette. This was necessary to reduce the influence of the forces due to surface tension, which could interfere with controlled positioning of the S.T. sensor. The S.T. sensor rod was held in a motorized micromanipulator, capable of undergoing prescribed 0.5-μm motions in three dimensions.

C. Stimulus delivery and response collection and analysis

1. Pressure measurements

Stimuli were pure tones, 32 ms in duration, with rise and fall times of 0.3 ms. The tones were generated at levels of 40, 60, and 80 dB SPL, as measured in the ear canal (see sound system calibration below), and frequencies of approximately 500 Hz, 1 kHz, 2 kHz, and then with a 2-kHz spacing to 46 kHz. The actual frequencies were adjusted from these values in order to coincide with the frequencies of the analysis FFT. In a series of S.V. pressure measurements made after the main data set the frequencies 188, 264, and 378 Hz were added. The earphone was a Radio Shack 40-1377 tweeter. Stimuli were generated and responses collected with a Tucker Davis Technologies (Gainesville, FL) DD1 using a 6.48-μs sampling rate. Typically 100 averages were taken, for total averaging times of 3.2 s. During ''simultaneous'' pressure measurements in the two scalae, actually the S.T. measurement followed the S.V. measurement, so the two occurred within approximately 7 s. The averaged data record of each response to each tone was stored for later analysis. The standard analysis was a FFT of the 4096 points of the data record beginning 5 ms into the record (point 805). The first 5 ms were truncated to exclude any transient response. The amplitude and phase at the stimulus frequency were extracted from the FFT. The complete FFT spectrum and raw data record was occasionally inspected. When plotting the phase as a function of frequency, ambiguity is handled by subtracting or adding 360 degrees or a multiple of it when the resultant phase differs from that of the adjacent lower frequency by less than ± 180 degrees.

2. CAP

Stimuli were pure tones, 3 ms in duration, with 0.3 ms rise/fall times. The polarity of alternate tones was reversed to cancel the cochlear microphonic in the averaged responses. The tones were generated at levels of 60, 80 and in later experiments also 40 and 100 dB SPL and frequencies of 2, 6, 10, 20, 30, and 40 kHz. Typically, 100 averages were taken. The averaged data records were displayed on line, and stored for later inspection. ''Threshold'' CAP is defined as the visible threshold, 5 to 10 μV peak-to-peak. The CAP was used as a monitor of cochlear condition (Johnstone *et al.*, 1979). Of particular interest are changes in the CAP after drilling the S.V. hole, after removal of the round window, and with time following opening the cochlea.

D. Sound system calibration

A 1-in. long earphone tube, coupled to the earphone via a machined housing, was inserted into the ear canal of the left ear following removal of the pinna. The bone of the bulla that overlies the tympanic ring and tapers down to form the ear canal contains natural cracks. A hole less than 1 mm in diameter was made in the skin-like tissue beneath one of the cracks, allowing access to the ear canal approximately 3 mm from the eardrum. A sensor was inserted approximately 1 mm into the hole and the hole was sealed with tissue paper reinforced by the slightly mucous fluids in the region. Tones generated with a constant voltage were delivered to the ear and the sensor's response to these tones was used to calibrate the sound system. Following calibration, 80 dB SPL tones at the standard frequencies were delivered to the ear, and recorded in order to check the magnitudes (which were 80 dB

Downloaded 30 Jun 2010 to 156.145.57.60. Redistribution subject to ASA license or copyright; see http://asadl.org/journals/doc/ASALIB-home/info/terms.jsp

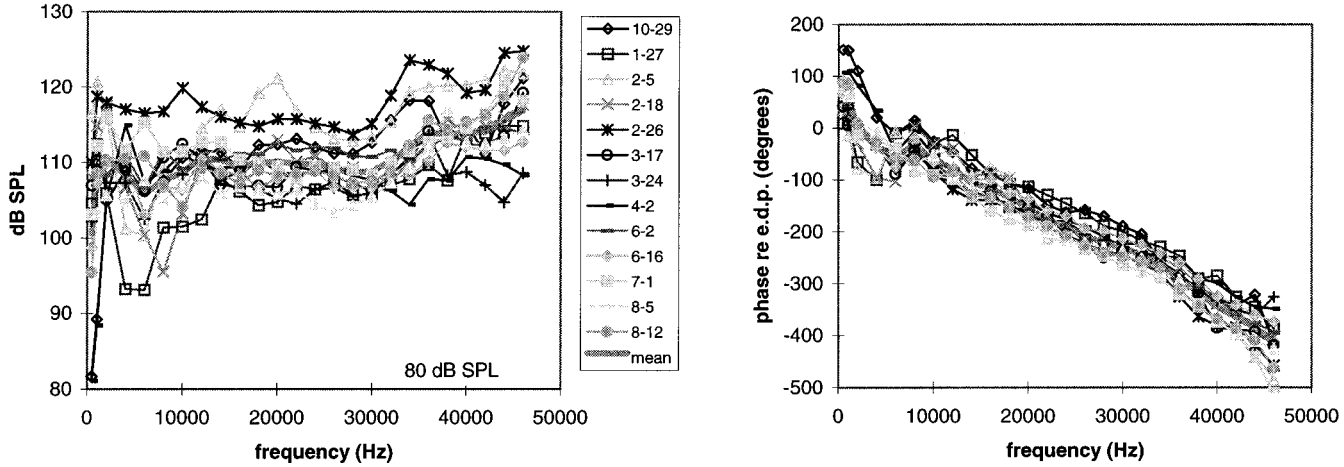

FIG. 5. The S.V. pressure with a stimulus level in the ear canal of 80 dB SPL; 500 Hz to 46 kHz. (a) Magnitude. (b) Phase relative to the pressure near the eardrum in the ear canal.

by construction) and to find the phase in the ear canal as a reference. The tissue paper was dampened to loosen it, the sensor removed, and the tissue paper replaced to cover the opening.

In two experiments following the set reported here the pressure field within the ear canal was mapped along the line between the sensor entrance and the umbo, a distance of approximately 3 mm, with a 0.5-mm resolution. The results of the two experiments were very similar. The detailed description of the results is beyond the scope of the present paper, but a brief description is relevant to the sound system calibration. At frequencies through 40 kHz the pressure close to the umbo was not more than 5 dB greater, and the phase at the umbo differed by at most -60 degrees, relative to the usual calibration position approximately 1 mm within the ear canal. At 46 kHz, the largest differences were seen. The magnitude at the umbo was 15 dB greater than at the usual calibration position and the phase differed by $-160°$.

E. Standard experimental sequence

(1) Sensors calibrated by immersion.
(2) Initial surgery, CAP electrode and earphone in place.
(3) Sensor 1 in ear canal, sound system calibration, CAP, recalibrate sensor 1.
(4) Scala vestibuli hole, CAP.
(5) Sensor 1 in scala vestibuli, pressure measurement, CAP, recalibrate sensor 1.
(6) Round window membrane removed, sensor 1 in S.V., sensor 2 in S.T., CAP, near simultaneous pressure measurements.
(7) Sensor 2 advanced towards B.M., pressure measured in both scalae after every 20- or 30-μm advance. CAP measured periodically.
(8) Sensor 2 contacted B.M., as determined by sensor 2 photodetector voltage, which undergoes abrupt increase in low frequency fluctuations.
(9) Sensor 2 retracted several micrometers, pressure measurements, CAP.
(10) Further measurements including post mortem measurements following anesthetic overdose.
(11) Sensors recalibrated.

II. RESULTS AND DISCUSSION

The results reported here are from 13 animals. The S.T. pressure data are not presented from all the experiments. In 6-16, 7-1, 8-5, and 8-12 S.T. pressure was not measured by design. In 10-29, 1-27, 2-5, and 2-18 it is not presented either because the B.M. was damaged during removal of the round window membrane, or because the S.V. and S.T. pressures were unstable. Instability was apparently caused by a changing round window fluid level or by an unvented ear canal.

A. CAP

The baseline CAP response was determined just after sound system calibration and prior to opening the cochlea, but with the bulla opened widely. The usual baseline CAP response was as follows: The CAP was visible at the lowest SPL (40 or 60 dB SPL) at 2, 6, 10, and 20 kHz. At 30 kHz the CAP was suprathreshold at 60 or 80 dB SPL, and at 40 kHz the CAP was suprathreshold at 80 or 100 dB SPL. Through 30 kHz, these results are in keeping with those of Müller (1996), who found (in his Fig. 1) a CAP threshold of 30 dB SPL at frequencies between 1 and 10 kHz, rising to 40 dB SPL at 20 kHz, and close to 60 dB SPL at 30 and 40 kHz. The 40 kHz threshold here is 20 dB higher than Müller's. The difference might be due to differences in method (electrode placement, sound system calibration, definition of ''threshold'') or to physiological changes in the extreme base related to the widely open middle ear.

Following drilling the S.V. hole, a change in sensitivity was always seen. Typically, both 30- and 40-kHz tones required one increment (20 dB) in sound level to be suprathreshold (a notable exception is experiment 2-26, in which the 30-kHz threshold was unchanged), whereas the CAP response to the 2- to 20-kHz tones was unchanged to the coarse degree measured. Following round window removal, the CAP response could be unchanged, and remain largely unchanged over hours of experimentation. A temporary threshold shift that might be due to the close proximity of the S.T. sensor to the B.M. occurred in experiment 2-26 (as described more fully below), and suggests that the sensor might indeed ''load'' the organ of Corti when positioned close to it.

Downloaded 30 Jun 2010 to 156.145.57.60. Redistribution subject to ASA license or copyright; see http://asadl.org/journals/doc/ASALIB-home/info/terms.jsp

B. Scala vestibuli input pressure

1. Grouped data

In Fig. 5 scala vestibuli pressure is shown when the sound level in the ear canal was set to 80 dB SPL. The measurements were made with the round window membrane intact. Figure 5(a) shows the pressure magnitude. In main, the S.V. input pressure lies between 105 and 120 dB SPL, indicating a middle ear pressure gain between 25 and 40 dB. The mean of the measurements (thick line without symbols) shows a frequency dependence which is flat at 110 dB SPL, a gain of 30 dB relative to the ear canal pressure, between 10 and 30 kHz, with a slight increase at the highest frequencies, and a slight decrease at the lowest frequencies. Some of this frequency dependence might be produced in part by experimental procedures. (i) High frequency increase: When fluid wells up in the round window, S.V. input pressure can increase by several dB, especially at high frequencies. In the data of Fig. 5, the round window membrane was intact, but the fluid level beneath the round window sometimes rose beneath the membrane when the cochlea was manipulated. Additionally, as discussed under ''sound system calibration'' above, the sound pressure in the ear canal which is used as a calibration might be underestimated at the highest frequencies. (ii) Low-frequency decrease, and structure: Sets 10-29 and 4-2 show a markedly low pressure at 0.5 and 1 kHz. The hole to S.V. was larger than optimal in the experiment of set 4-2. This is expected to reduce the pressure, especially at low frequencies. (Notes on the hole size from set 10-29 were not made.) Sets 1-27, 2-5 and 2-18 show dips in the 5- to 10-kHz region. These experiments were performed without a vent to the ear canal, an unnatural condition which can lead to buildup of static pressure. In the experiments following 2-18, a vent was purposely maintained, and the structure in the 5- to 10-kHz regions is less apparent in the later experiments. The variability from experiment to experiment is due in part to errors in sensor calibration, which might be up to 6 dB (see sensor notes above). In the mid-frequency region, where systematic errors due to calibration uncertainties, fluid level and static pressure are least apparent, the interexperiment spread is 12 dB, so calibration errors could account for much of the variability. The magnitude data indicates that the gain of the middle ear is approximately 30 dB, and is fairly flat with frequency above 2 kHz. The phase of S.V. input pressure relative to the pressure in the ear canal shows a linear decrease with frequency. The linear phase can be expressed as a delay which, in this case, accumulating one cycle between 2 and 42 kHz, is 25 μs. *Thus, both the magnitude and phase indicate that, at frequencies above 2 kHz, the middle ear and its cochlear termination have the properties of a frequency-independent transmission line.* From a signal processing standpoint, this is a good system, because the temporal qualities of the input are preserved in the output. Other investigators have noted a transmission-line-like character of the middle ear, based on measurements of middle ear impedance (Puria and Allen, 1997) and middle ear motion (Decraemer *et al.*, 1997).

In Fig. 6, results from five later experiments are shown in which the frequency range was extended down to 188 Hz.

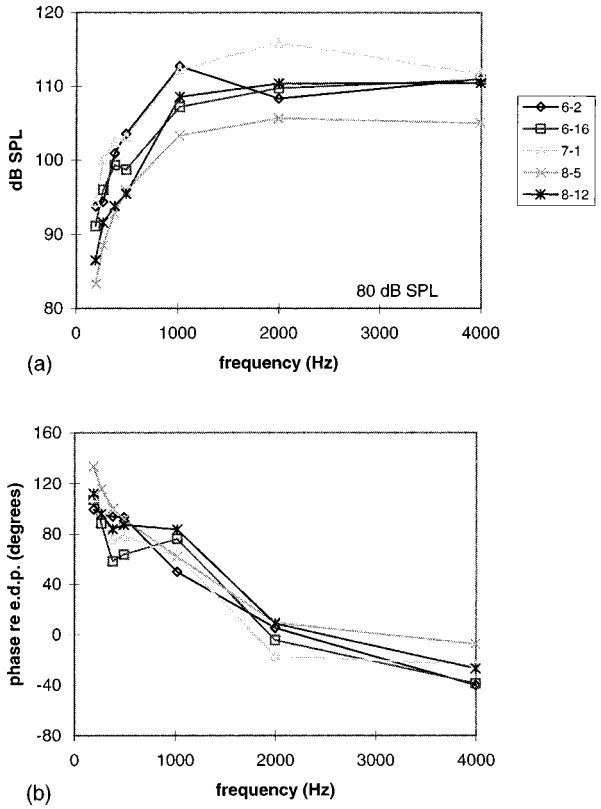

FIG. 6. The S.V. pressure with a stimulus level in the ear canal of 80 dB SPL; low-frequency extension. In these cochleae, measurements were made at the usual frequencies, and at three additional low frequencies. Here responses are only shown through 4 kHz to emphasize the low frequency behavior. (a) Magnitude. (b) Phase relative to the pressure near the eardrum in the ear canal.

The gain of the middle ear decreased as frequency decreased below 2 kHz, and was approximately 10 dB at 188 Hz. The phase relative to the pressure within the ear canal was approximately 0 degrees at 2 kHz, and increased as frequency decreased. At 188 Hz it ranged between 95 and 115 degrees in four experiments, and in the fifth was 135 degrees.

2. Comparison with previous measurements of basal S.V. pressure

Basal S.V. pressure has been measured *in vivo* by others (guinea pig, Dancer and Franke, 1980; cat, Nedzelnitsky, 1980; cat, chinchilla and guinea pig, Decory *et al.*, 1990). The variations in amplitude and phase at frequencies below 2 kHz and the maximal gain value of approximately 30 dB here adhere to the standard pattern that has been reported. However, the frequency range over which the 30 dB gain obtains is relatively large. Specifically, there is no indication that the gain comes down at high frequencies. Presumably, it comes down at high enough frequencies, but through 46 kHz (well within the hearing range of the gerbil) the gain is fairly steady, at 30 dB, at frequencies above 1 kHz. This finding *is* in agreement with Dancer and Franke's 1980 measurements in guinea pig turn 1, which showed a gain that was within a few dB of 32 dB between the frequencies of 1 and 20 kHz,

Downloaded 30 Jun 2010 to 156.145.57.60. Redistribution subject to ASA license or copyright; see http://asadl.org/journals/doc/ASALIB-home/info/terms.jsp

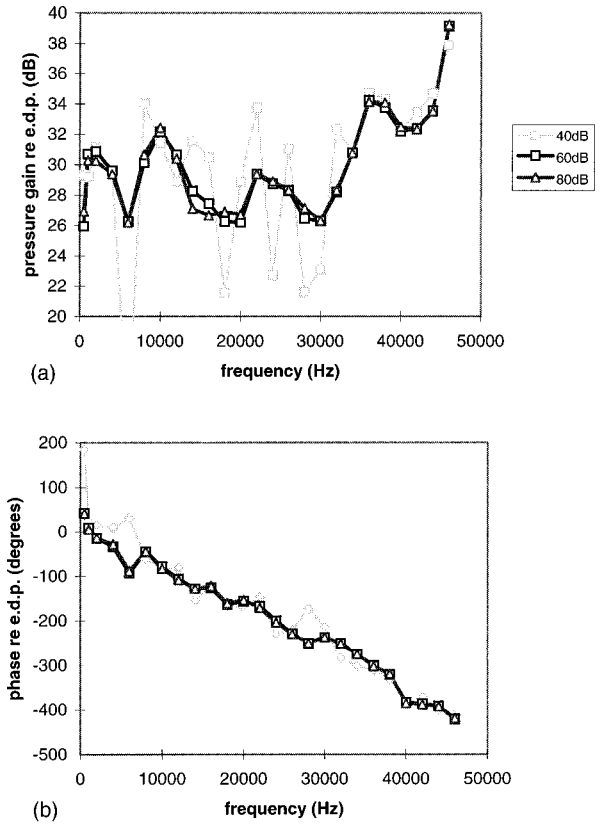

FIG. 7. Linearity in the S.V. pressure. (a) Scala vestibuli pressure gain relative to ear canal pressure at SPLs of 40, 60 and 80 dB. (b) The S.V. pressure phase relative to the pressure near the eardrum in the ear canal. One experiment is shown for clarity (3-17), but the linearity in evidence was common to all measurements of S.V. input pressure. The responses to the 40-dB stimulus were close to the noise floor.

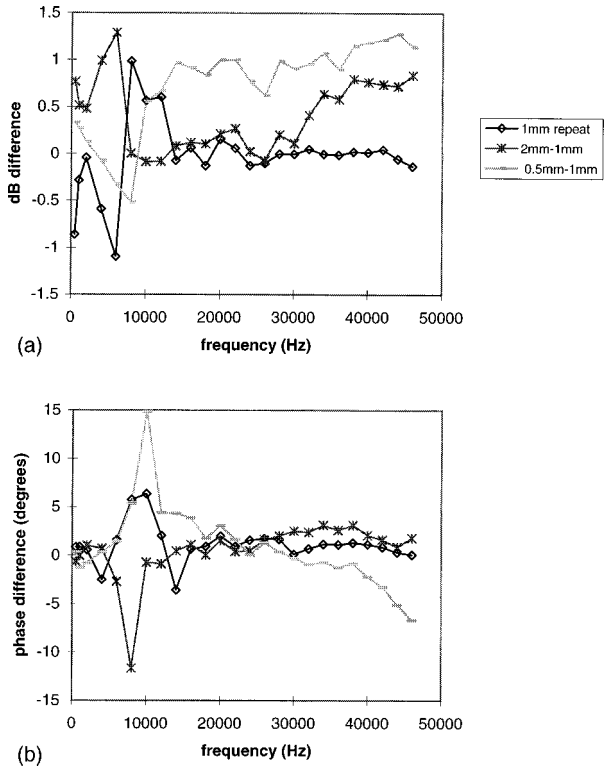

FIG. 8. Changes in S.V. pressure with changes in the insertion depth of the S.V. sensor (expt 2-18). The S.V. pressure appears relatively insensitive to millimeter-sized changes in insertion depth. As indicated in the legend, the changes are plotted (i) between two repeated measurements, both at a depth of 1 mm, (ii) between the initial 1-mm measurement and a measurement with a 2-mm insertion, and (iii) between the initial 1-mm measurement and a measurement with a 0.5-mm insertion. (a) Magnitude changes. (b) Phase changes.

the highest frequency they measured. However, most previous reports find a reduction in gain beginning at frequencies around 10 kHz. For example, the basal S.V. pressure measured by Decory *et al.* dropped off markedly at frequencies above 14 kHz (chinchilla), 12 kHz (guinea pig) and 8 kHz (cat). The measurements were made 5.5 (chinchilla), 7.2 (guinea pig) and 8 (cat) mm from the extreme base; perhaps the high-frequency S.V. pressure changes substantially over these distances. Puria *et al.* (1997) show a drop off in basal S.V. pressure at frequencies above about 8 kHz in human temporal bones, but the report states that temporal bone preparations might not be comparable with live preparations at frequencies above 5 to 10 kHz. The phase data reported here are in keeping with those of others, for example, Dancer and Franke (1980), who reported a phase of approximately +90 degrees at 1 kHz, decreasing monotonically to −200 degrees at 20 kHz.

3. Linearity

In Fig. 7 the scala vestibuli pressure gain and phase relative to the pressure in the ear canal are shown for 40, 60 and 80 dB SPL stimuli. The results from 3-17 are displayed. The gains at 60 and 80 dB lie essentially on top of each other, and at 40 dB are basically the same, but are so close to the noise floor that a strict comparison is not possible. The linearity illustrated applies to all measurements of S.V. input pressure.

4. Variations with insertion depth

The position of measurement in scala vestibuli does not allow for the sensor to be inserted much further than 1 mm without potential harm to the saccule. For this reason, generally the sensor was inserted less than 1 mm and variations in S.V. pressure due to insertion depth were not explored. One case in which the insertion depth variation *was* explored (2-18) is illustrated in Fig 8. In Fig. 8(a), the differences in measured SPL are displayed, and in Fig. 8(b), the differences in phase. The changes are small, and show no clear position dependence. The S.V. pressure appears to be relatively insensitive to millimeter-sized changes in insertion depth.

5. The effect of removing the round window membrane

Following round window membrane removal, the S.V. pressure usually changed very little, less than 2 or 3 dB. When fluid welled up in the round window opening the S.V. pressure sometimes increased, especially at the highest frequencies. The changes were typically less than 5 dB.

Downloaded 30 Jun 2010 to 156.145.57.60. Redistribution subject to ASA license or copyright; see http://asadl.org/journals/doc/ASALIB-home/info/terms.jsp

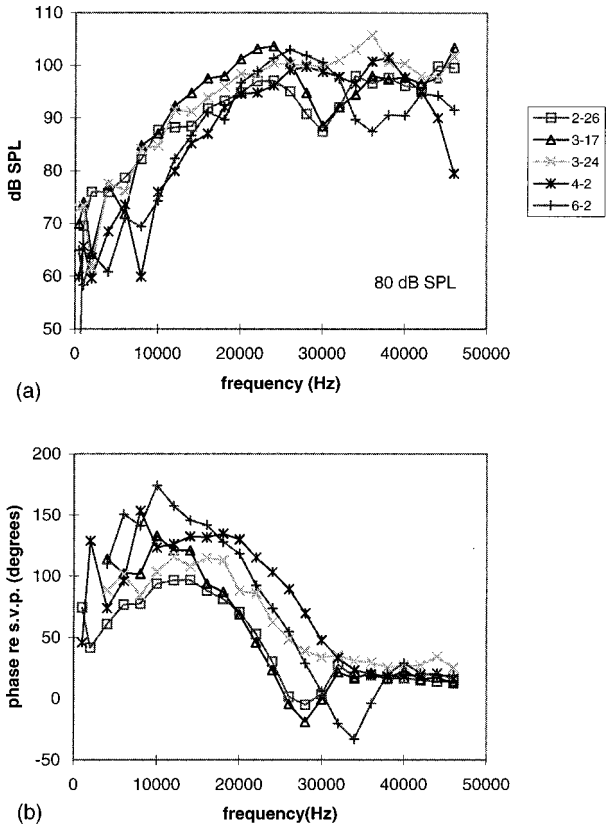

FIG. 9. The S.T. pressure with a stimulus level in the ear canal of 80 dB SPL. Shown are the initial S.T. measurements, made prior to the approach to the B.M. The distances from the B.M. are not known precisely, but are estimated as between approximately 300 and 800 μm. (a) Magnitude. (b) Phase relative to the simultaneously measured S.V. pressure.

6. Abnormal conditions

Data collected following severe manipulations to the middle ear, whether intentional or unintentional, serve as controls for systematic errors in the form of electronic cross-talk. In an early experiment the ossicles were suspected damaged during drilling of the S.V. hole and an air bubble was inadvertently introduced into S.V. The S.V. pressure gain (relative to the ear canal pressure) was 5 dB at the lowest frequency, and decreased steadily with frequency to -20 dB at 20 kHz, where the pressure went beneath the noise floor. These manipulations are known to decrease scala vestibuli pressure (Nedzelnitsky, 1980; Puria *et al.*, 1997). At the end of one experiment the annular ligament was purposely broken. The S.V. pressure gain was reduced at all frequencies to approximately 0 dB.

C. Scala tympani pressure

In the phase data in the figures below S.T. pressure is referenced to the simultaneously measured S.V. pressure.

1. Grouped data

In Fig. 9 scala tympani pressure is presented from five animals. The following conditions are of note: At the time of the presented measurements the CAP thresholds were relatively healthy in 2-26, 3-24, and 6-2, but were elevated more than 20 dB at all frequencies in 3-17 and 4-2. In 3-24 a portion of the round window membrane was covering the B.M. basal to the measurement position, and in 4-2 the round window membrane was covering all accessible regions of the B.M., including the region where measurements were made.

Figure 9(a) shows the magnitude of the S.T. pressure when the sensor was initially positioned into scala tympani. The stimulus level in the ear canal was 80 dB SPL. Recall that the c.f. in this region is thought to be in the neighborhood of 30 kHz. The distance from the B.M. is not known precisely, but in all cases is estimated as between 300 and 800 μm. The pressure increases with frequency from approximately 70 dB SPL (-10 dB *re:* ear canal pressure) at 4 kHz to approximately 100 dB SPL ($+20$ dB *re:* ear canal pressure) at 24 kHz. The pressure contains notches and peaks in the region of the c.f.

The phase relative to simultaneously measured scala vestibuli pressure is shown in Fig. 9(b). At the lowest frequencies the phase is erratic in part because the magnitudes were close to the noise floor. In general the phase lies between 50 and 100 degrees at 5 kHz, increases about 50 degrees to a maximum slightly above 10 kHz and then decreases to close to 0 degrees at the highest frequencies. In the region around 30 kHz a phase dip is evident in experiments in which pronounced structure is apparent in the magnitude data.

2. Variations in S.T. pressure as B.M. is approached

In Figs. 10–13 S.T. pressure versus position with 80 dB SPL stimuli is shown for experiments 2-26, 3-24 and 3-17 pre-mortem, and 2-26 post-mortem. In experiment 6-2 the fluid drained out of the round window opening while the B.M. was being approached, and a pressure versus position series was not possible. The magnitude and phase showed little change with position in experiment 4-2. As described above, in this experiment the round window membrane had not been successfully removed, and was between the sensor and the B.M. Based on the 4-2 results, the membrane probably prevented the sensor from making a close approach to the B.M., and might have modified the intracochlear fluid motions.

Figure 10 shows S.T. pressure versus position from 2-26 pre-mortem. The numbers in the legend indicate the distance from the B.M. in micrometers. The order of the measurements advances from top to bottom, but are not all consecutive. (Consecutive measurements were spaced by 20 to 30 μm; not all are shown.) After the measurement 28 μm from the B.M. was recorded the sensor was advanced 28 μm, where it contacted the B.M. and was retracted approximately 3 μm. Following the measurement there, the sensor was retracted 20 μm for the final measurement of this series. The similarities between the measurements 23 and 28 μm from the B.M. attests to the experimental stability. In general, the scala tympani pressure increased as the B.M. was approached, although the region of notches displays a non-monotonic increase. Below 10 kHz and above 38 kHz the pressure changes were relatively small. The pressure changes were most striking in the 30-kHz region. Figure 10(c) reinforces these points by displaying the pressure as a function of position from the B.M. for five frequencies. Figure 10(b) illustrates the 2-26 S.T. pressure phase, referenced to simul-

Downloaded 30 Jun 2010 to 156.145.57.60. Redistribution subject to ASA license or copyright; see http://asadl.org/journals/doc/ASALIB-home/info/terms.jsp

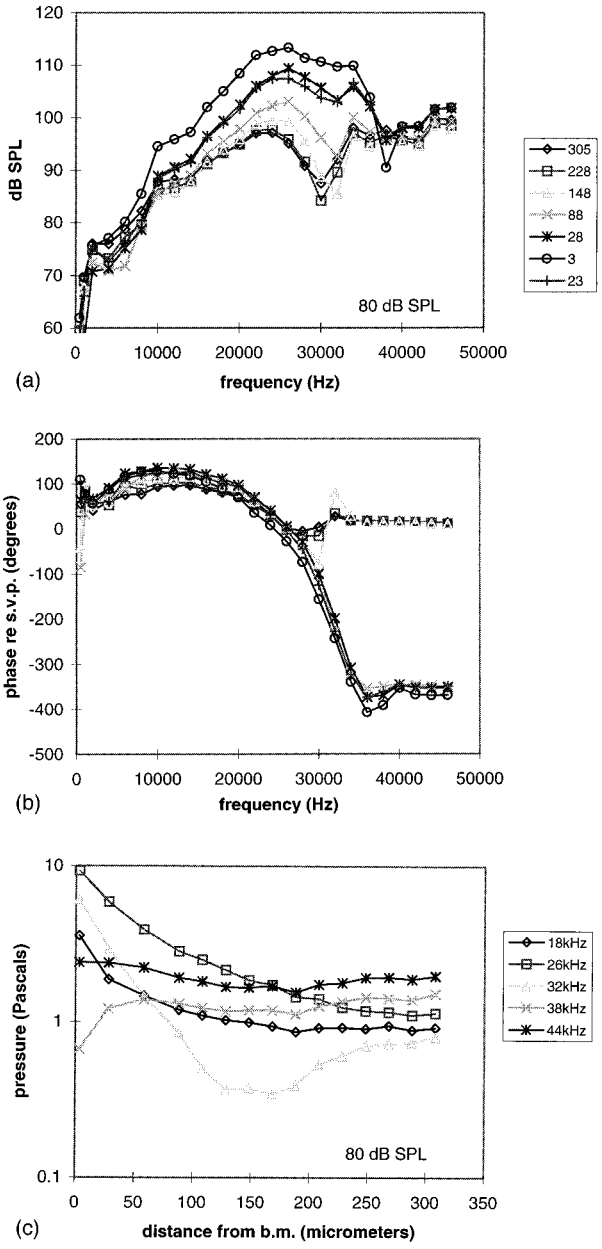

FIG. 10. The S.T. pressure, with a stimulus level in the ear canal of 80 dB SPL, as the B.M. was approached (expt. 2-26). The legend indicates the distance of the sensor from the B.M. in micrometers. The order of the measurements advances from legend top to legend bottom. (a) Magnitude. (b) Phase relative to the simultaneously measured S.V. pressure. (c) Magnitude plotted as a function of distance from the B.M. at selected frequencies.

taneous S.V. pressure. The phase dip/rise in the 30-kHz region becomes more and more pronounced until, when the distance to the B.M. is approximately 100 μm, it is appropriate to unwrap it. This reveals the phase as advancing, accumulating more than 500 degrees.

In Fig. 11 S.T. pressure versus position is shown from 3-24. The numbers in the legend indicate the distance from the B.M. in micrometers, and are from consecutive measurements beginning with the 84-μm position. A prominent notch at 22–24 kHz becomes deeper as the B.M. is approached. The phase exhibits dips and peaks in the same range of frequencies. At the position closest to the B.M. the

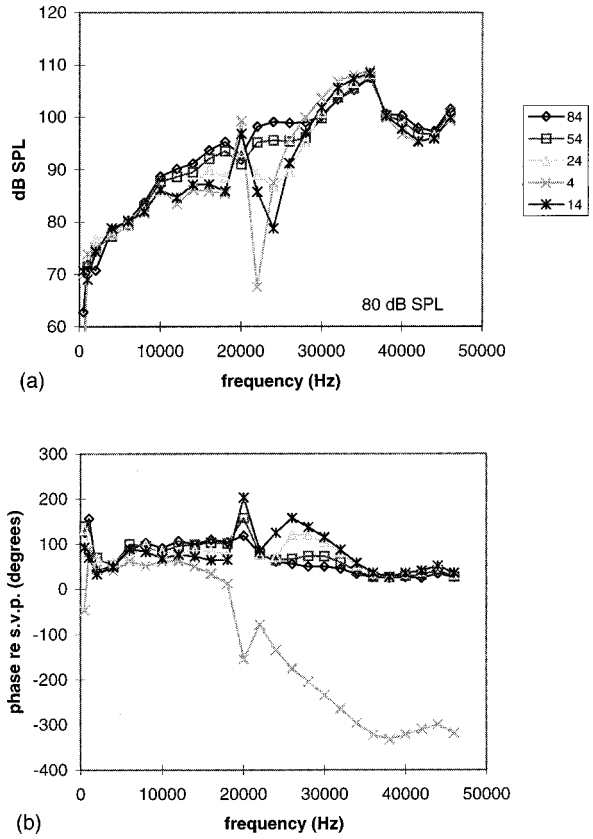

FIG. 11. The S.T. pressure, with a stimulus level in the ear canal of 80 dB SPL, as the B.M. was approached (expt. 3-24). The legend indicates the distance of the sensor from the basilar membrane in micrometers. The order of the measurements advances from legend top to legend bottom. (a) Magnitude. (b) Phase relative to the simultaneously measured S.V. pressure.

phase accumulates more than 370 degrees between 4 and 38 kHz. It is notable that at most frequencies between 10 and 24 kHz, the magnitude of the pressure decreased as the B.M. was approached.

In Fig. 12 S.T. pressures from 3-17 are shown at three different positions. Difficulties with surface tension prevented well-controlled positioning of the S.T. sensor in this experiment and the positions are only approximate, as the figure legend indicates. In general the pressure increased as the B.M. was approached. At the closest position, the phase accumulates almost 500 degrees.

Following the measurement 23 μm from the B.M. in experiment 2-26 (Fig. 10) the sensor was retracted an additional 20 μm, and the animal was administered a lethal dose of anesthetic. Just post-mortem pressure versus position was again recorded. Figure 13 shows these measurements, at distances 42, 22, and 2 μm from the B.M. The closest measurement was made after contacting the B.M., and retracting the sensor 2 μm.

In summary, as the B.M. was approached the S.T. pressure magnitude generally increased but sometimes decreased, typically in frequency regions where notches were present. The amount of phase accumulation with frequency increased as the B.M. was approached.

Downloaded 30 Jun 2010 to 156.145.57.60. Redistribution subject to ASA license or copyright; see http://asadl.org/journals/doc/ASALIB-home/info/terms.jsp

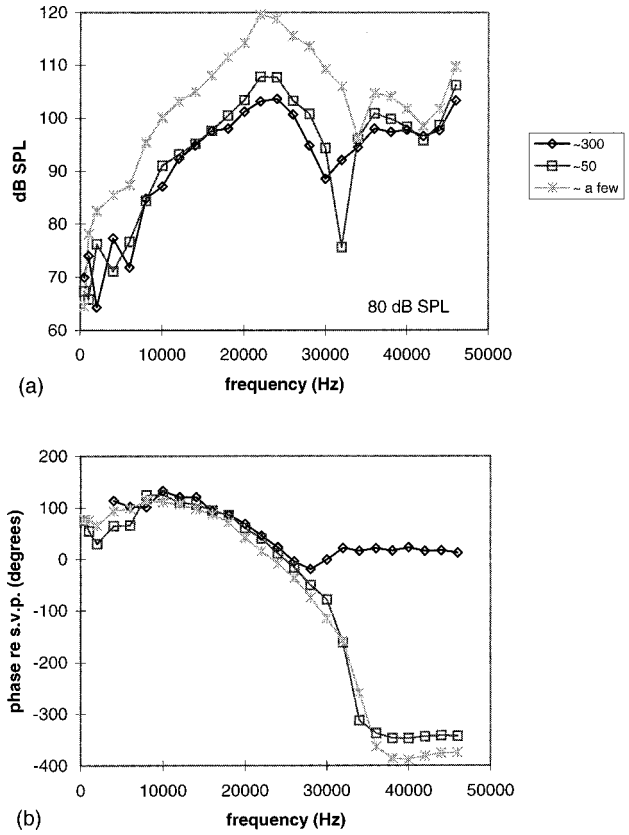

FIG. 12. The S.T. pressure, with a stimulus level in the ear canal of 80 dB SPL, as the B.M. was approached (expt. 3-17) The forces due to surface tension prevented well-controlled positioning in this experiment and the legend indicates the approximate distance from the basilar membrane in micrometers. The order of the measurements advances from legend top to legend bottom. (a) Magnitude. (b) Phase relative to the simultaneously measured S.V. pressure.

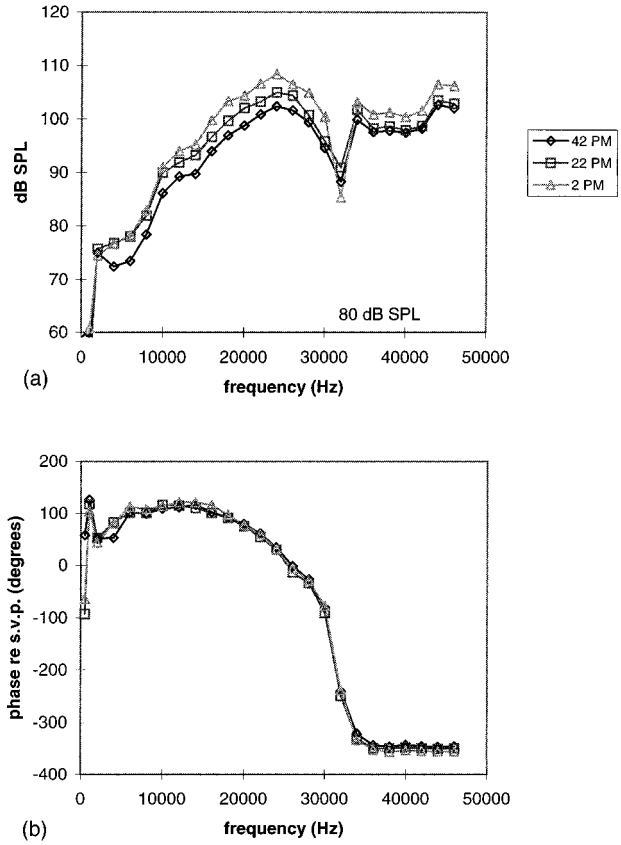

FIG. 13. The S.T. pressure, with a stimulus level in the ear canal of 80 dB SPL, as the B.M. was approached (expt. 2-26 postmortem). Following the measurement 23 μm from the B.M. in Fig. 10 the sensor was retracted an additional 20 μm, and the animal was administered a lethal dose of anesthetic. The measurements here were made immediately post-mortem. The legend indicates the distance of the sensor from the basilar membrane in micrometers. (a) Magnitude. (b) Phase relative to the simultaneously measured S.V. pressure.

3. Discussion of notches, peaks and phase accumulation

The pronounced notches in the magnitude data, and the position-dependent phases of Figs. 10–13 can be interpreted as the interaction of two pressure modes: a fast mode whose phase changes little with frequency, and a slow traveling wave mode whose accumulating phase chronicles the wave's travel. Interpreted in this framework, the notches in the magnitude data are produced by interference between the two modes. At frequencies where the modes are out of phase they sum destructively, and if their magnitudes are similar notches appear. The phase data indicate which mode is dominant: the fast mode is dominant in the data of Fig. 9(b), far from the B.M. As the B.M. is approached, the slow mode can dominate, producing a phase that accumulates smoothly with frequency. The transition region between the two modes can be quite erratic.

Fast and slow modes are explicit in mathematical models, where slow modes are associated with the traveling wave motion of the organ of Corti complex and fast modes are required to satisfy the boundary conditions. In a 1-D model, one fast and one slow mode suffices (Peterson and Bogart's P+ and P−, 1950). In 2-D and 3-D models more than one fast mode is present (Taber and Steele, 1981). Perhaps there are several slow modes as well (Taber and Steele, 1981; Hubbard, 1993). The emergence of phase accumulation as the B.M. is approached can be related to modeling predictions. At all but low frequencies, and more-so as frequency is increased, the pressure of the slow wave is predicted to be localized close to the B.M. (Lighthill, 1981; Taber and Steele, 1981). The S.T. pressure is predicted to be largest at frequencies near the peak of the traveling wave, and to penetrate the scalae a distance on the order of the traveling wave wavelength. (The penetration distance is the distance at which the traveling wave pressure is reduced from its value at the B.M. by roughly a factor of e.) This penetration distance is estimated from Taber and Steele's figure 7 (1981) as about 100 μm at 10 kHz, near the position where 10 kHz was the c.f. (Their model was based on guinea pig, and was passive with an orthotropic B.M.) In Fig. 10(b) (2-26) at distances relatively far from the B.M. substantial phase accumulation is not apparent, indicating that the fast wave is dominant. Within 88 μm of the B.M., similar to the predicted penetration depth of the slow wave, phase accumulation is apparent, indicating that the slow wave pressure has become dominant. Thus, this modeling prediction is in rough agreement with the data.

Referring to phase data where the slow mode is dominant, the phase versus frequency slope is much less steep

Downloaded 30 Jun 2010 to 156.145.57.60. Redistribution subject to ASA license or copyright; see http://asadl.org/journals/doc/ASALIB-home/info/terms.jsp

between 10 and 20 kHz than between 20 and 36 kHz. At the lowest frequencies, the sign of the slope is reversed. Traveling wave models predict that the phase versus frequency slope becomes steeper as frequency increases towards c.f., with details of the increase dependent on the impedance of the O.C. complex (e.g., Taber and Steele, 1981; Neely and Kim, 1986). Still, traveling wave models do not predict a low-frequency reversal in phase slope. A possible explanation for the behavior lies in the relative strengths of the fast and slow modes. At frequencies much lower than c.f. the traveling wave is expected to be small, and S.T. pressure even close to the B.M. is likely dominated by the fast mode. Then the phase is not expected to accumulate. The fast mode probably dominates at frequencies above c.f. as well, where models predict there is no longer a traveling wave. At frequencies above c.f. the measured phase-frequency slope is close to zero.

4. Interanimal variability

Although there are basic similarities in the S.T. data from different cochleae, there are some clear differences. The notches and peaks appear at different frequencies. In 2-26 (Fig. 10) the phase changes smoothly with large accumulation at positions 88 μm from the B.M. and closer, whereas in 3-24 (Fig. 11) the phase shows a *reasonably* smooth accumulation at the closest position, 4 μm from the B.M., but even 14 μm from the partition it is not appropriate to unwrap it. The reasons for the variability probably fall into two basic categories. First, the S.T. pressure probably depends on the basic condition of the cochlea. The condition is known to some degree, and based on the cochlear conditions noted when discussing Fig. 9 it is evident that the phase accumulation that signifies the dominance of the slow mode can be present post-mortem (from 2-26PM), and in experiments with elevated CAP threshold (from 3-17). When the round window membrane is unnaturally positioned on top of the B.M. it might obscure the slow mode (from 4-2) or alter it (from 3-24).

The second categorical reason for experimental variability is that S.T. pressure was not measured at identical points in different animals. Due to experimental variability in the portion of the RW membrane that was successfully removed, and the exact positioning of the animal in the stereotaxic frame and relative to the sensor apparatus, the angle of the sensor varied, its longitudinal position varied, and its radial position varied. The resulting positional variations are probably on the order of 200 μm. This distance is significant in these measurements, where S.T. pressure was found to vary by a factor of 10 over distances of 100 μm. Referring to the theoretical literature, in a 3-D model Taber and Steele (1981) predict that at a distance 100 μm from the B.M. the magnitude of the slow mode pressure at a radially centered location is more than twice that of the slow mode pressure over the pillar cells. Closer to the B.M., the predicted difference is much greater. Therefore, a pressure measurement made over the pillar cells is expected to be substantially different than one made over the pectinate zone. In short, the scala tympani measurements from different animals cannot be regarded as precisely repeated measurements.

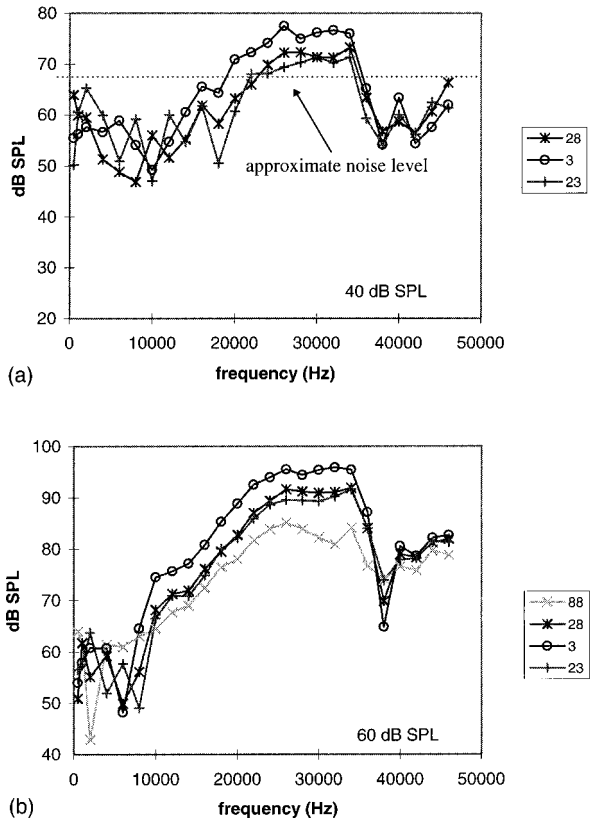

FIG. 14. Scala tympani pressure, with stimulus levels in the ear canal of 40 and 60 dB SPL, as the B.M. was approached (expt. 2-26). The data are from the same experimental run as the data in Fig. 10.

5. Comparison with previous measurements

The S.T. data can be compared with measurements of Dancer and colleagues, who have presented basal scala tympani pressure measurements from guinea pigs. Our measurements relatively far from the B.M. (Fig. 9) are similar to the recent publication in which Dancer *et al.* (1997) find the S.T. pressure to peak in the region close to the c.f. (10 kHz in their case) with a gain relative to ear canal pressure close to 20 dB. Those measurements found little phase difference between S.T. and S.V. pressures: a small lead at low frequencies, and a small lag at the highest measured frequencies, just over 10 kHz. Due to this lack of phase accumulation, Dancer *et al.* take an extreme viewpoint, and question the presence of a traveling wave pressure at all. However, an earlier publication (Dancer and Franke, 1980) reported S.T. pressure with a larger gain (up to 40 dB near 10 kHz), suggesting that it was measured closer to the B.M. than the measurements presented later. In this case, the phase of S.T. relative to S.V. did exhibit phase accumulation, from 90 to -270 degrees between 500 and 12 000 Hz. The results here include these two extremes, and illustrate the progression between them.

6. Linearity, expt. 2-26

In Fig. 14, the magnitude data recorded in the same run as that of Fig. 10 are shown for 40 and 60 dB SPL stimuli. The noise floor is at a measured pressure of approximately 65 dB SPL, restricting the frequency ranges over which the data are reliable. The S.T. pressures scale almost linearly.

Downloaded 30 Jun 2010 to 156.145.57.60. Redistribution subject to ASA license or copyright; see http://asadl.org/journals/doc/ASALIB-home/info/terms.jsp

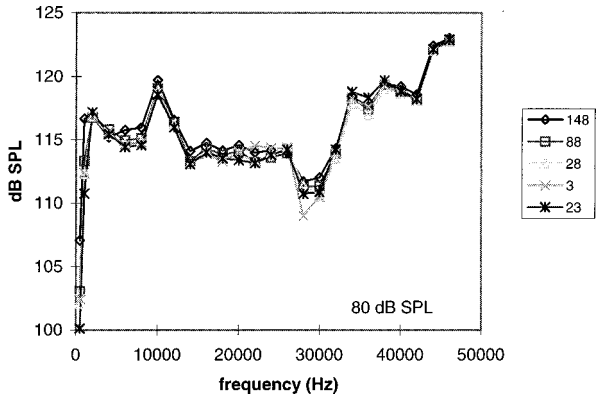

FIG. 15. Scala vestibuli pressure measured when the S.T. sensor was at distances from the B.M. indicated in the legend (expt. 2-26). The stimulus level in the ear canal was 80 dB SPL. Changes in S.V. pressure due to the proximity of the S.T. sensor to the B.M. indicate that the S.T. sensor was loading the cochlea.

However, the profiles differ from each other slightly in the c.f. region, particularly comparing the data taken with the stimulus levels at 60 and 80 dB SPL. At 32 kHz the departure from linearity is maximal, approximately 8 dB at positions close to the B.M.

7. Simultaneous scala vestibuli pressure, and pressure changes with changing position of S.T. sensor

A pressure change in S.V. due to S.T. sensor proximity to the B.M. could indicate that the S.T. sensor was ''loading'' the system. Fig. 15 displays the S.V. pressure measured as the S.T. sensor approached the B.M. Distances from the B.M. in micrometers are listed in the legend and occurred consecutively starting at the 148-μm position. A 3-dB dip in S.V. pressure occurred close to the c.f. when the sensor was closest to the B.M., suggesting that the sensor perturbed the pressure field. The S.V. pressure is measured far from the O.C.; the S.V. pressure close to the O.C. was presumably perturbed more. The change at very low frequencies is not linked to the position of the S.T. sensor but is increasing in time. It might be due to a slowly widening gap between the S.V. sensor and the hole to S.V.

III. ANALYSIS: DERIVED QUANTITIES

In this section the results are analyzed to estimate the velocity of the B.M, the pressure across the organ of Corti complex, and the specific acoustic impedance of the organ of Corti complex. The derivation was sketched previously (Olson and Borawala, 1997) and is presented here in the Appendix. The analysis is carried out for experiments 3-24 and 2-26. In both these experiments the overall CAP thresholds were relatively low (particularly in 2-26) and the scala tympani pressure measurements close to the B.M. were checked for repeatability, ruling out time-dependent changes in S.T. pressure as a source of error.

There are numerous measurements of basal B.M. velocity in the literature, and the general form of its frequency dependence has been documented under various physiological conditions (Cooper and Rhode, 1992a, 1992b; Nuttall and Dolan, 1996; Xue *et al.*, 1995; Khanna and Leonard, 1986; Ruggero *et al.*, 1996, 1997). That the derived B.M. velocity is similar to the B.M. velocity measured by direct methods serves as an important measure of the reliability of the current analysis. By this measure, the analysis of experiment 2-26 will be found to be the most credible. Because of the lack of high-quality data from more experiments, the primary purpose of the current presentation is to establish the analytical method.

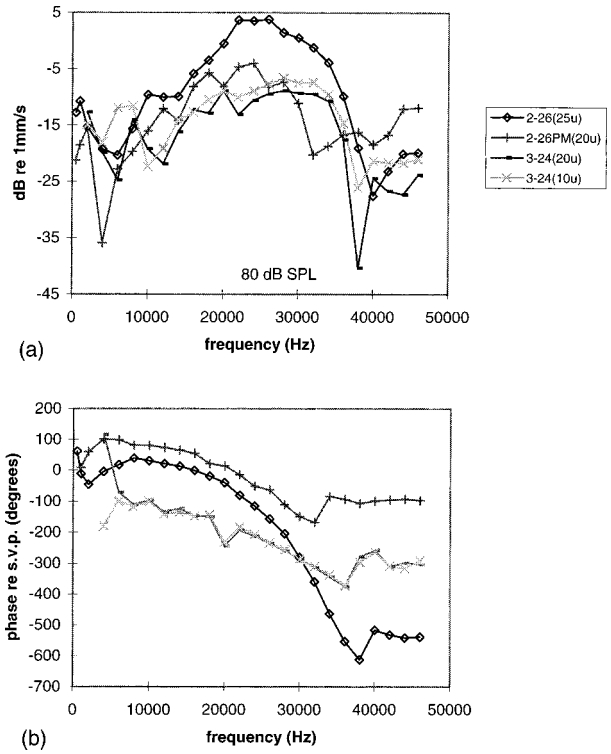

FIG. 16. Derived B.M. velocity from experiments 3-24 and 2-26. The stimulus level in the ear canal was 80 dB SPL. The velocities are derived from pairs of S.T. pressure measurements. 2-26(25u) is derived from the S.T. pressure 3 μm, and the previous measurement 28 μm, from the B.M. 2-26PM(20u) was derived from the S.T. pressure 2 μm, and the previous measurement 22 μm, from the B.M. 3-24(20u) was derived from the S.T. pressure 4 μm, and the previous measurement 24 μm, from the B.M. 3-24(10u) was derived from the S.T. pressure 4 μm, and the following measurement 14 μm, from the B.M. Phases are referenced to the S.V. pressure measured simultaneously with the S.T. pressure of closest approach. A phase of 0 degrees indicates velocity towards scala tympani.

A. Basilar membrane velocity

1. Results from two animals, discussion of derivation method

Figure 16(a) displays the magnitude of the B.M. velocity calculated from 2-26 and 3-24. Figure 16(b) shows the velocity phase relative to S.V. pressure. A phase of 0 degrees indicates velocity towards scala tympani. The stimulus level was 80 dB SPL in the ear canal. As described in the Appendix, fluid velocity is calculated from a pair of consecutive S.T. pressure measurements, where one member of the pair is the pressure closest to the B.M. The B.M. velocity is then equated to this fluid velocity, based on the argument that close to the B.M. the fluid must move with the B.M. The S.T. pressure measurements used in these calculations are in

Downloaded 30 Jun 2010 to 156.145.57.60. Redistribution subject to ASA license or copyright; see http://asadl.org/journals/doc/ASALIB-home/info/terms.jsp

Figs. 10 (2-26), 11 (3-24) and 13 (2-26PM). The two 3-24 velocities in the figure were derived from two such pairs, one comprised of the pressure at the closest position and the pressure at the previous position (20-μm distant), and one comprised of the pressure at the closest position and the pressure at the following position (10-μm distant). Figure 16's legend specifies the distance between the measurements within a pair. The differences between the 3-24 results with 10- or 20-μm separation are generally small, indicating that the results are not extremely sensitive to changes in this distance.

The derived velocities are similar in: (i) their broadly peaked shapes, (ii) the positions of their maxima, which vary from 24 to 28 kHz, (iii) the absolute values of their maxima, which vary from 0.3 to 1.6 mm/s, and (iv) dropping off relatively sharply at a frequency above their maxima. The phases from the different measurements all decrease with increasing frequency at a steadily increasing rate above about 8 kHz, then level off at approximately the frequency where the corresponding amplitude drops off. Although the phase shows these basic similarities, the amount of phase accumulation and the value of the phase at both low and high frequencies varies substantially. Experiments 2-26PM and 3-24 show much less phase accumulation (approximately 270 degrees in both cases) than 2-26, which accumulates more than 600 degrees. Although similar in overall phase accumulation, the 3-24 and 2-26PM phases are offset from each other by close to 180 degrees at all frequencies. Referring to the S.T. pressure data that was used to derive the velocities, the underlying reasons for the 180-degree difference can be investigated. The phase offset originates in the unusual behavior of the 3-24 pressure, which over a wide range of frequencies was smaller at the position closest to the B.M. than at the position one step back. Only in the region of the maximum, 28–36 kHz, does the pressure convincingly increase as the B.M. was approached. This observation shifts the question from ''Why are the velocities different?'' to ''Why does the pressure decrease as the B.M. is approached?'' In fact, a decrease in S.T. pressure as the B.M. was approached was evident in all experiments. The decrease occurred in association with a notch, and is thought to originate in interference between the fast and slow modes. In 3-24 the decrease is associated with a notch in the frequency range from 20–26 kHz, somewhat lower than the position of the prominent notch in the other experiments. The significance of 3-24's lower notch frequency, as well as of the unusually large frequency extent of the decrease is not known. The behavior was repeatable within this approach and in a second approach in this animal, ruling out a confounding influence of time-dependent changes. As noted previously, S.T. sensor positioning was not optimal in 3-24 because a portion of the basal B.M was covered with the remains of the round window membrane. Perhaps the S.T. pressure was perturbed by the unnatural condition of the basal B.M.

The S.T. pressure data that underlies the velocity calculation indicates the frequency regions over which the derived velocity is most reliable. Because velocity is derived from the pressure differences between two consecutive positions, its derived value is most robust at frequencies for which (i) the pressure was well above the noise level, (ii) the differences with position were substantial, and (iii) the pressure was only position dependent, and not changing over time. The first of these requirements is most restrictive at low frequencies. The second requirement is most restrictive at frequencies above those where the velocity drops off, because the pressure differences are small while the levels are relatively high. The third requirement underscores the need for measurements both before and after contacting the B.M. to ascertain repeatability. For data sets 3-24 and 2-26 the repeatability was documented. Although time-dependent changes (due to fluid level changes for example) were not noted when set 2-26PM was collected, it was not deliberately checked for repeatability.

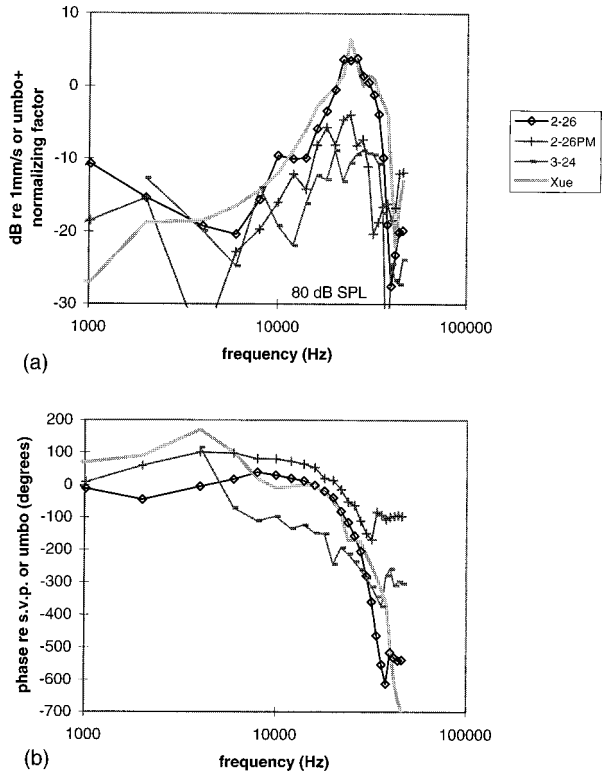

FIG. 17. Derived B.M. velocity at a stimulus level of 80 dB SPL replotted on a logarithmic scale, along with results from Xue *et al.* (1995) at 90 dB SPL. 3-24(10u) has been excluded to reduce clutter. (a) Magnitude. (Xue *et al.*'s magnitude data were referenced to umbo motion and are shifted vertically to line up with the 2-26 data.) (b) Phase. (Xue *et al.*'s phase is referenced to umbo velocity.)

2. Comparison with direct velocity measurements

In Fig. 17 the velocities are plotted on a logarithmic frequency scale to facilitate comparison with the B.M. motion literature. Included in the figure is Xue *et al.*'s (1995) direct measurement of gerbil B.M. velocity, made through the open round window, and taken with the stimulus level at 90 dB SPL. Xue *et al.*'s B.M. velocity is reported relative to umbo velocity. The derived B.M. velocity is found with a constant SPL in the ear canal, and its phase is reported relative to S.V. input pressure. Although the references are different, above 2 kHz Xue *et al.*'s data can be directly compared to the derived velocity based on the following: (i) From the S.V. pressure results here, the gain of the S.V. pressure relative to the pressure in the ear canal is approxi-

Downloaded 30 Jun 2010 to 156.145.57.60. Redistribution subject to ASA license or copyright; see http://asadl.org/journals/doc/ASALIB-home/info/terms.jsp

mately flat with frequency above 2 kHz. (ii) The cochlear input impedance is approximately resistive above 2 kHz (Lynch *et al.*, 1982; Puria and Allen, 1991). (iii) The umbo and stapes move in phase (Ruggero *et al.*, 1990). When these three conditions are met, the magnitude of the derived B.M. velocity (referred to pressure in the ear canal) and the magnitude of B.M. velocity (referred to umbo motion) can be plotted together, with an offset which on a log scale is an additive constant. (The constant is treated as free parameter.) When (ii) and (iii) are met the phase of the derived B.M. velocity (referred to S.V. pressure near the stapes) and the phase of the B.M. velocity (referred to umbo velocity) are equivalent, and can be plotted together with no free parameters. Actually, at high frequencies (ii) and (iii) are not known to hold. Lynch *et al.*'s measurements of cochlear input impedance only extend through about 7 kHz. With regards to (iii), although Ruggero *et al.* (1990) showed that the malleus and stapes moved almost in phase up to about 8 kHz, at higher frequencies the stapes velocity lagged malleus velocity. At approximately 20 kHz, the phase lag could be as large 130 degrees. The complexity of ossicle motion at high frequencies has been noted by others as well (e.g., Decraemer *et al.*, 1994). Therefore, the different references might sully the comparison somewhat, but a correction is not attempted. What is presented in Fig. 17 is a straight comparison with Xue *et al.*'s data, in which there is one free parameter, which is used to move Xue *et al.*'s magnitude data along the vertical axis so that the peaks line up. The form of the 2-26 derived velocity is similar to that measured by Xue *et al.* The agreement lends credibility to the general method of deriving B.M. velocity with pressure differences. The values of the derived velocity magnitudes are close to that found in basal locations of the chinchilla and guinea pig at stimulus levels of 80 dB SPL (Ruggero *et al.*, 1997; Sellick *et al.*, 1982), and the variation with frequency of both the magnitude and phase of the derived velocity 2-26 is in keeping with what has been reported in many studies in addition to that of Xue *et al.* (e.g., Cooper and Rhode, 1992a; Nuttall and Dolan, 1996). The phases of 2-26PM and 3-24 do not possess the multiple cycles of phase accumulation that is characteristic of B.M. motion. However, similarly small accumulations can be found in the B.M. motion literature. For example, Cooper and Rhode found less than one cycle of phase accumulation between 10 and 40 kHz, measuring at the 30-kHz place in guinea pig (1992a) and in linear cat cochleae (1992b).

3. Linearity, expt. 2-26

In Fig. 18 the 2-26 results at 40, 60 and 80 dB SPL are shown. The 40- and 60-dB data have been scaled by factors of 100 and 10, respectively, as indicated in the *y*-axis title. Results are shown within the frequency ranges for which S.T. pressure was out of the noise. At all SPLs, the maximum occurred at 26 kHz. The velocity scaled nearly linearly with sound pressure, but compression at frequencies on the high-frequency side of the peak extended the peak through relatively higher frequencies (32 kHz) at 40 and 60 dB SPL. The observation that the nonlinearity is very modest is not surprising since high-frequency CAP thresholds were elevated slightly when the cochlea was opened. Additionally, when the S.T. sensor was closest to the B.M., the CAP threshold at 30 kHz was temporarily elevated from 60 to 80 dB SPL. When the sensor was retracted 20 μm, the 60-dB response at 30 kHz recovered. The degree to which pressure measurements like those here can explore cochlear activity, and the associated nonlinearity, without interfering with it, is not yet established.

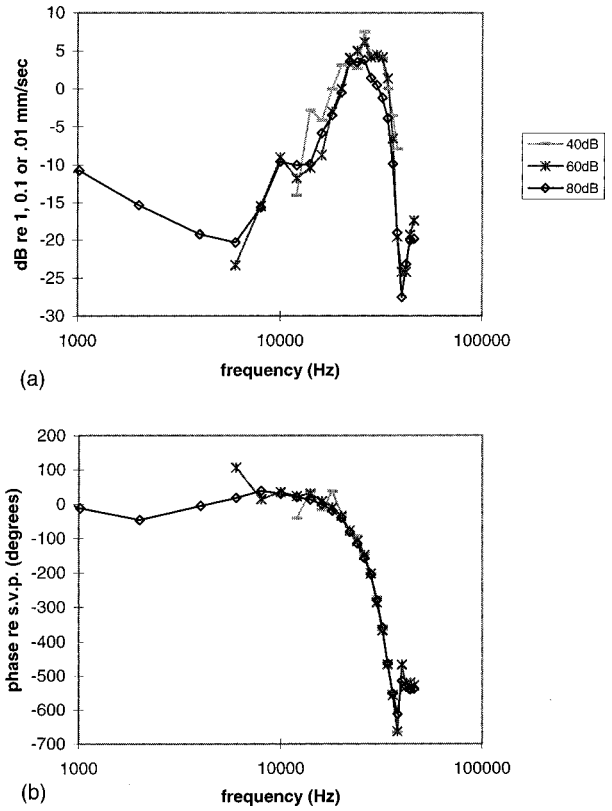

FIG. 18. Derived B.M. velocity from experiment 2-26 at stimulus levels of 40, 60 and 80 dB SPL. (a) Magnitude. The results at 40, 60 and 80 dB SPL are plotted *re*: 0.01 mm/s, 0.1 mm/s, and 1 mm/s, respectively. (b) Phase relative to S.V. pressure.

B. Localized pressure difference across the organ of Corti complex

1. Results

The derivation of the local pressure difference across the organ of Corti complex, ΔP_{oc}, is in the Appendix. In Fig. 19 ΔP_{oc} is shown. Pre-mortem, ΔP_{oc} values calculated from 2-26 (40, 60 and 80 dB SPL) and 3-24 show a mild peak in the region of c.f. A small degree of nonlinearity is in evidence in the 2-26 results. In ΔP_{oc} calculated from 2-26PM the pressure peak is absent, and a pronounced notch is apparent. Most notably, in all the results, ΔP_{oc} is not small at frequencies above c.f., where the velocity was small.

In Fig. 19(b) the phase is shown relative to the S.V. pressure. At low and high frequencies, the phase is close to 0 degrees (or 360 degrees), simply because the S.V. pressure was much greater than the S.T. pressure. Pre-mortem in experiment 2-26, between 14 and 34 kHz, the phase accumulates almost 500 degrees. The results from 2-26 PM and 3-24 show only the beginning of phase accumulation, similar to

Downloaded 30 Jun 2010 to 156.145.57.60. Redistribution subject to ASA license or copyright; see http://asadl.org/journals/doc/ASALIB-home/info/terms.jsp

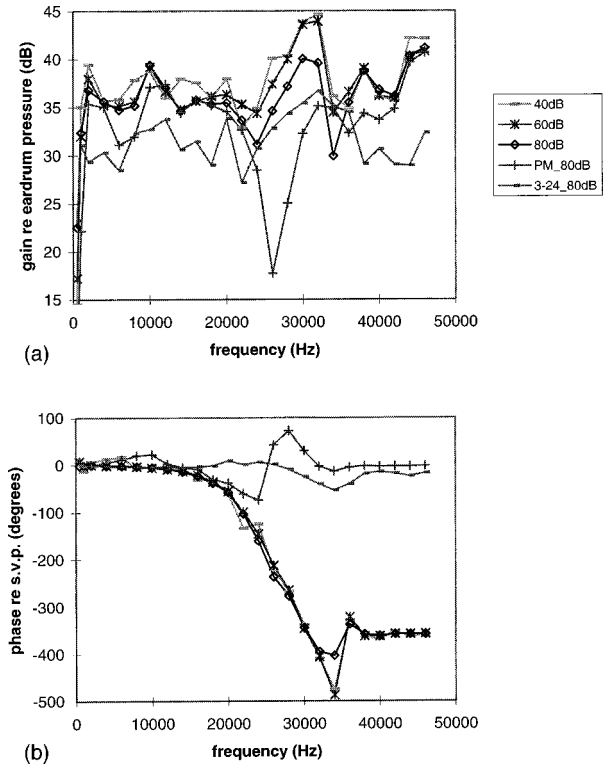

FIG. 19. Derived pressure across the O.C. complex, ΔP_{oc}, from experiments 2-26 and 3-24. The stimulus level was 40, 60 or 80 dB SPL as indicated in the legend. ΔP_{oc} is equal to the pressure on the S.V. side of the O.C. complex minus the pressure on the S.T. side of the O.C. complex. (a) Magnitude. (b) Phase relative to S.V. pressure.

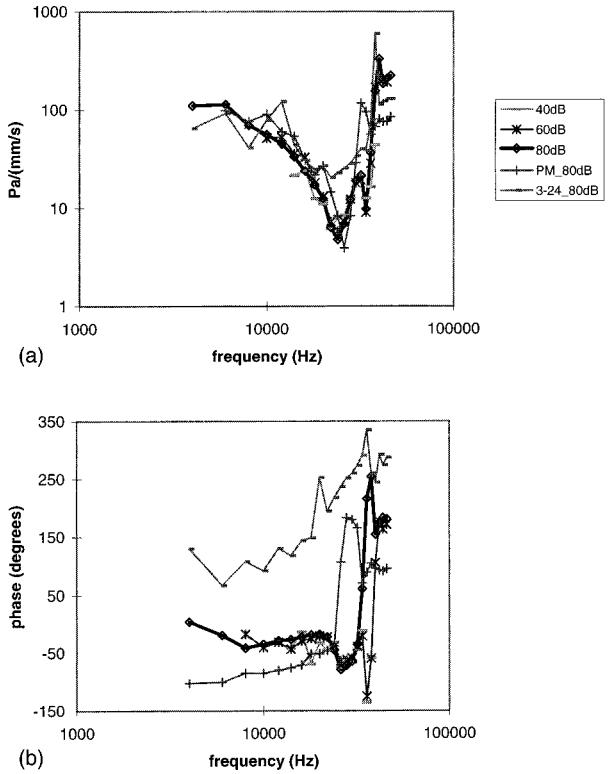

FIG. 20. The specific acoustic impedance of the organ of Corti. Results are shown at stimulus levels of 40, 60 or 80 dB SPL, as indicated in the legend. (a) Magnitude=ΔP_{oc}/B.M. velocity. (b) Phase=ΔP_{oc} phase−B.M. velocity phase.

the velocity measurements of these approaches. The basis for the difference in 2-26 ΔP_{oc} post-mortem compared to pre-mortem lies in the S.T. pressure close to the B.M. The S.T. pressure was larger pre-mortem, and the phase decreased through the c.f. region more smoothly pre-mortem than post-mortem, indicating that the slow mode was relatively dominant. The quantitative change in the relative strengths of the fast and slow pressure modes pre- versus post-mortem resulted in a qualitative change in the character of ΔP_{oc}.

2. Discussion

Similarly to S.T. pressure, ΔP_{oc} appears to be composed of the sum of a fast and a slow mode. The significance of the fast mode is undoubtedly emphasized in the current measurements, made at a position sandwiched between the stapes and round window. At longitudinal positions apical to the windows, presumably the fast mode of ΔP_{oc} is smaller. On the other hand, the significance of the fast mode of ΔP_{oc} to cochlear mechanics should not be undervalued. A sizable fraction of the O.C. complex lies in the region between the windows (Plassman *et al.*, 1987), and is close to the round window membrane; the anatomy of the cochlea does not seem to be set up to protect the O.C. complex from being effectively stimulated by the fast mode.

Based on point pressure measurements not particularly close to the B.M. Dancer *et al.* (1997) concluded that ΔP_{oc} did not have a traveling wave mode. The results here do not substantiate this view, but they do support a milder form of the contention of Dancer *et al.*: that the traveling wave pressure is not the only pressure across the O.C. complex, and, moreover, that it is not always the dominant pressure.

C. Specific acoustic impedance of the organ of Corti

1. Results

In Fig. 20 the magnitude and phase of the specific acoustic impedance is shown for experiments 3-24 and 2-26. Its derivation is in the Appendix. The impedance magnitude is tuned to frequencies between 22 and 26 kHz. Its size is approximately 100 Pa/(mm/s) at low (6 kHz) and high (approximately 40 kHz) frequencies, and at its minimum is approximately 5 Pa/(mm/s) in experiment 2-26, and 20 Pa/(mm/s) in experiment 3-24. The 2-26 pre-mortem impedances at 40, 60 and 80 dB SPL show a primary minimum at 24 kHz, with a secondary minimum close to half an octave above at 32 kHz. These impedances nearly overlie each other; the small degree of compressive nonlinearity evident in 2-26 ΔP_{oc} and 2-26 velocity cancel each other.

2. Discussion

The impedance phase of a simple mechanical resonance begins at −90 degrees at low frequencies, rises through 0 degrees at the resonance frequency, and ends up at +90 degrees. The post-mortem 2-26 data do that, except for an overshoot to +180 degrees just beyond the resonance. The pre-mortem 2-26 impedance phase is more complicated, with a low-frequency plateau at −30 degrees, a slight decrease to −70 degrees in the region of the magnitude's primary minimum, and a notch and peak at higher frequencies. Compared

Downloaded 30 Jun 2010 to 156.145.57.60. Redistribution subject to ASA license or copyright; see http://asadl.org/journals/doc/ASALIB-home/info/terms.jsp

to the 2-26 data, the 3-24 phase shows a large offset. This offset is produced by the phase of the 3-24 velocity, which is in turn rooted in the large frequency extent over which S.T. pressure decreased as the B.M. was approached.

In the ''low-frequency'' region from 6 to 12 kHz, the slope of the magnitude curve is nearly constant, at −6 dB/oct, both pre- and post-mortem in experiment 2-26. Experiment 3-24 decreases less smoothly. A 6-dB/oct decrease is expected for a stiffness dominated impedance. In phase, a pure stiffness is constant, at −90 degrees. Post-mortem 2-26 the impedance phase is close to −90 degrees between 6 and 12 kHz, but the pre-mortem 2-26 approach has a phase close to −30 degrees, suggesting that at these frequencies the impedance is a combination of stiffness and damping. The viscoelasticity of biological tissue is capable of producing an impedance with the low-frequency character of the pre-mortem data (Fung, 1993). The specific acoustic stiffness indicated is approximately 2 Pa/nm (pre-mortem approach), or 6 Pa/nm (post-mortem approach). These compare favorably with the point stiffness found by direct methods, 7 N/m for a 20-μm probe tip (Olson and Mountain, 1994), which translates to a specific acoustic stiffness of 4 Pa/nm (Olson and Mountain, 1991).

It is generally believed that *in vivo* the impedance is active in some sense — that the O.C. pumps energy into the traveling wave (de Boer, 1983; Diependaal *et al.*, 1986). To date, however, direct experimental probes of activity have not been able to substantiate its existence (Allen and Fahey, 1992; Cody, 1992). With respect to this important question the results here are not very helpful. A driving point impedance without negative real components must have a phase between +90 and −90 degrees; a phase beyond these limits indicates that the real part of the impedance is negative. Although the 2-26 impedance phases are somewhat interpretable in the framework of what is predicted for a resonant impedance, at frequencies near c.f. the phase is most aptly described as erratic. This undoubtedly stems in part from an oversimplified analysis; the phase is more sensitive than the magnitude to the simplifications imposed by the analytical method, particularly the assumption that the ΔP_{oc} we derive corresponds spatially exactly to the v_{bm} we derive. Further measurements and possibly more sophisticated analyses are required to address the question of activity.

Computer models (Steele and Taber, 1979; Steele, 1974) demonstrated that frequency selectivity in the cochlea could be present without a tuned O.C. impedance. In these models the O.C. complex is an acoustic stiffness whose value decreases apically. The slow mode (which propagates with the traveling wave) is essentially the only pressure across the O.C. complex in the models; the fast mode pressure across the complex is negligible except very close to the base. The models predict that the slow mode pressure peaks and then dies out at frequency-dependent longitudinal positions along the O.C. The motion of the O.C. will die out, resonant impedance or not, when its stimulus dies out. Physical models of the cochlea have demonstrated this inherent tuning (Zhou *et al.*, 1993). Most computer models incorporate a tuned O.C. impedance which enhances the peak of the traveling wave and steepens the drop off at frequencies above c.f. In

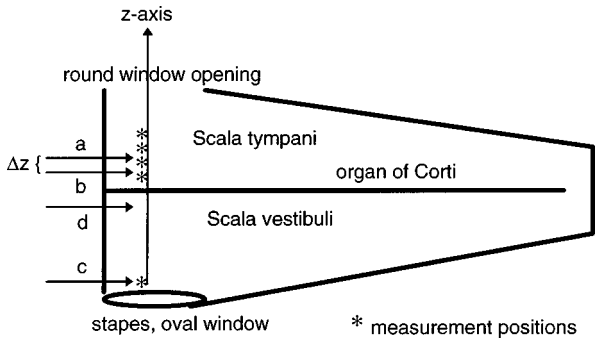

FIG. 21. Symmetric cochlear model. The asterisks indicate positions where pressure is measured. B.M. velocity is derived from measured pressures P_a and P_b . $\Delta P_{\mathrm{oc}} = P_d - P_b$ is derived from measured pressures P_b and P_c , and an assumption that the pressure at the round window is 0.

all these models the pressure difference across the O.C. complex is carried by the traveling wave and dies out at frequencies above c.f. (Peterson and Bogart, 1950; Taber and Steele, 1981; Neely and Kim, 1986; Kolston, 1988).

The results here indicate that in the base of the gerbil cochlea the pressure difference across the organ of Corti does not die out at frequencies above the characteristic frequency. The slow mode of ΔP_{oc} dies out, but the fast mode remains sizable. Therefore, the current analysis argues that in the extreme base, tuning in the impedance of the O.C. complex is doing the job, not just of enhancing the response of the O.C. complex near c.f., but of attenuating the response at frequencies above c.f. as well.

IV. CONCLUSION

The detailed form of the fluid pressure within the cochlea is governed by the motion of its boundaries. One of these boundaries is the stapes, and the cochlear pressure adjacent to the stapes is key to understanding the workings of the middle ear. In this vein, the results of the current study extend previous studies to higher frequencies and support the view that over a wide range of frequencies the middle ear operates as a transmission line. Another, more elusive cochlear boundary in motion is the organ of Corti. Because it both drives and responds to the motion of the O.C. complex, the fluid pressure encodes fundamental information about the O.C.'s mechanical properties. In this study, the signature of the O.C.'s motion was apparent in the slow wave dominated S.T. pressure close to the B.M. A simple method for extracting the specific acoustic impedance of the O.C. from the pressure field indicated that the impedance is tuned.

ACKNOWLEDGMENTS

Sejal Borawala, as a research intern at Rutgers/Newark, helped develop the first sensor tips. Shuwan Xue generously shared his basilar membrane motion data. Joe Santos-Sacchi, Dana Anderson, Reg Cook, Betsy Keithley and Mike Ravicz advised in various technical matters. Bob Austin made room for me in his lab at Princeton. Discussions with the scientists at Boston University, the Eaton Peabody Laboratory and Rockefeller University influenced the manuscript, and Dave Mountain's comments on its first version stimulated many revisions. I am very grateful to the JASA reviewers, John

Downloaded 30 Jun 2010 to 156.145.57.60. Redistribution subject to ASA license or copyright; see http://asadl.org/journals/doc/ASALIB-home/info/terms.jsp

Rosowski and a second reviewer who remained anonymous. This work was supported by N.I.H. Grant No. DC03130. Initial sensor development was supported by a Visiting Professorship for Women from the N.S.F.

APPENDIX: DERIVED QUANTITIES

The analysis refers to the symmetric cochlear model in Fig. 21. In the formulation, pressures and velocities are complex quantities with a harmonic time dependence, $e^{i\omega t}$.

1. B.M. velocity

The difference between two adjacent S.T. pressure measurements was used to estimate the vertical (z) component of the pressure gradient. From this the z component of fluid velocity was found. Close to the B.M. (within about 30 μm, a fraction of the width of the B.M.) the fluid is assumed to move with the B.M. because of conservation of fluid mass. Therefore, the fluid velocity just adjacent to the B.M. is an approximate measure of B.M. velocity. In the quantitative derivation below, the following are used: ρ is fluid density, assumed similar to that of water, 10^3 kg/m^3; μ is the viscosity of the fluid, taken as that of water, 10^{-3} kg/(m-s); ∇ represents the gradient operator, which is written in component form as $\nabla = \partial/\partial x i + \partial/\partial y j + \partial/\partial z k$; P_a and P_b are the pressures measured at the two positions closest to the B.M., a and b in Fig. 21; v is the fluid velocity; v_z is its vertical component, and $v_{\rm bm}$ is the velocity of the B.M. As the sketch indicates, the positive z-axis points from the stapes towards the round window.

Here, L, U, and ω are scale factors used to characterize the fluid system, with the purpose of simplifying its mathematical description. L is the extent over which fluid velocities vary appreciably (nominally, by a factor of e), and it is taken as 100 μm, half the width of the basilar membrane. U is the maximum characteristic velocity of the basilar membrane and the fluid, and is taken as 1 mm/s, while ω represents the angular frequency (2π frequency), and is taken as 10^4, which is a conservative value for frequencies above 1.5 kHz.

The Navier–Stokes equation (A1) describes the relationship between fluid pressure gradients and fluid motion in an incompressible fluid:

$$\nabla P = -\rho \frac{\partial v}{\partial t} + -\rho v \cdot \nabla v + \mu \nabla^2 v. \tag{A1}$$

The relative sizes of the three terms involving fluid velocity can be estimated using the standard tools of dimensional analysis. Using L, U and ω we write v, t and spatial derivatives as dimensionless quantities, and Eq. (A2) is rewritten in terms of dimensionless coefficients:

$$\left(\frac{L}{\mu U}\right)\nabla P = -\left\{\frac{L^2\omega\rho}{\mu}\right\}\frac{\partial \mathrm{v}}{\partial \mathrm{t}} - \left\{\frac{UL\rho}{\mu}\right\}(\mathrm{v}\cdot\nabla \mathrm{v}) + \{1\}\nabla^2 \mathrm{v}. \tag{A2}$$

In Eq. (A2) all roman quantities are dimensionless (v, t, and ∇). The bracketed coefficients are also dimensionless, and by comparing their sizes, the dominant velocity term is identified. $\{L^2\omega\rho/\mu\}=100$ and $\{UL\rho/\mu\}=0.1$. Because the first coefficient is much larger than the other two coefficients, only the first velocity term is retained in this analysis.

Therefore, (A2) is simplified as

$$\nabla P = -\rho \frac{\partial v}{\partial t}. \tag{A3}$$

We are interested in the z component:

$$\frac{\partial P}{\partial z} = -\frac{\rho \partial v_z}{\partial t} \approx \frac{(P_a - P_b)}{\Delta z}, \tag{A4}$$

$$\therefore \frac{\partial v_z}{\partial t} = -\frac{(P_a - P_b)}{(\rho \Delta z)}. \tag{A5}$$

For pressures with a harmonic time dependence

$$v_z = (i/\omega)(P_a - P_b)/(\rho \Delta z). \tag{A6}$$

Finally, just adjacent to the B.M., $v_{\rm bm} \approx v_z$, so we assume

$$\boldsymbol{v_{bm} = (i/\omega)(P_a - P_b)/(\rho \Delta z)}. \tag{A7}$$

2. Local pressure difference across the organ of Corti complex

In a symmetric cochlea [Eq. (A1)] the z components of fluid motion are the same on both sides of the organ of Corti complex. Pressure gradients in the z direction indicate the z component of the fluid motion. The total pressure difference from the round window to the B.M. will be equal to the total pressure difference from above the organ of Corti complex in scala vestibuli to the oval window:

$$P(rw) - P(b) = P(d) - P(c). \tag{A8}$$

We assume that $P(rw) = 0$, and measure $P(b)$ and $P(c)$. We want

$$\Delta P_{\rm oc} = P(d) - P(b). \tag{A9}$$

From Eqs. (A8) and (A9)

$$\boldsymbol{\Delta P_{oc} = P(c) - 2P(b)}. \tag{A10}$$

3. Specific acoustic impedance of the organ of Corti complex

The magnitude of the acoustic impedance is found as $|\mathbf{\Delta P_{oc}/v_{bm}}|$. The phase of the impedance is found

$$\boldsymbol{(\Delta P_{oc}\ \ phase) - (v_{bm}\ \ phase)}. \tag{A11}$$

Allen, J., and Faley, P. (**1992**). ''Using acoustic distortion products to measure the cochlear amplifier gain on the basilar membrane,'' J. Acoust. Soc. Am. **92**, 178–188.

de Boer, E. (**1983**). ''No sharpening? A challenge for cochlear mechanics,'' J. Acoust. Soc. Am. **73**, 567–573.

Cody, A. (**1992**). ''Acoustic lesions in the mammalian cochlea: Implications for the spatial distribution of the 'active process,' '' Hearing Res. **62**, 166–172.

Cooper, N. P., and Rhode, W. S. (**1992a**). ''Basilar membrane mechanics in the hook region of cat and guinea-pig cochlea: Sharp tuning and nonlinearity in the absence of baseline position shifts,'' Hearing Res. **63**, 163–190.

Cooper, N. P., and Rhode, W. S. (**1992b**). ''Basilar membrane tonotopicity in the hook region of the cat cochlea,'' Hearing Res. **63**, 191–196.

Cooper, N. P., and Rhode, W. S. (**1996**). ''Fast travelling waves, slow travelling waves, and their interactions in experimental studies of apical cochlear mechanics,'' Aud. Neurosci. **2**, 207–212.

Downloaded 30 Jun 2010 to 156.145.57.60. Redistribution subject to ASA license or copyright; see http://asadl.org/journals/doc/ASALIB-home/info/terms.jsp

Dancer, A., and Franke, R. (**1980**). ''Intracochlear sound pressure measurements in guinea pigs,'' Hearing Res. **2**, 191–205.
Dancer, A., Avan, P., and Magnan, P. (**1997**). ''Can the traveling wave be challenged by direct intracochlear pressure measurements?,'' in *Diversity in Auditory Mechanics*, edited by E. R. Lewis, G. R. Long, R. F. Lyon, P. M. Narins, C. R. Steele, and E. Hecht-Poinar (World Scientific, Singapore), pp. 340–346.
Decory, L., Franke, R. B., and Dancer, A. L. (**1990**). ''Measurement of middle ear transfer function in cat, chinchilla and guinea pig,'' in *The Mechanics and Biophysics of Hearing*, edited by P. Dallos, C. D. Geisler, J. W. Matthews, M. A. Ruggero, and C. R. Steele (Springer Verlag, Berlin), pp. 270–277.
Decraemer, W. F., Khanna, S. M., and Funnell, W. R. J. (**1994**). ''A method for determining three-dimensional vibration in the ear,'' Hearing Res. **77**, 19–37.
Decraemer, W. F., Khanna, S. M., and Funnell, W. R. J. (**1997**). ''Vibrations of the cat tympanic membrane measured with high spatial resolution,'' Abstract 192 from the 20th Midwinter Research Meeting, Association for Research in Otolaryngology.
Diependaal, R. J., Viergever, M. A., and deBoer, E. (**1986**). ''Are active elements necessary in the basilar membrane impedance?,'' J. Acoust. Soc. Am. **80**, 124–132.
Fung, Y. C. (**1993**). *Biomechanics: Mechanical Properties of Living Tissues*, 2nd ed. (Springer Verlag, New York), Chap. 7.
Hu, A., Cuomo, F. W., and Zuckerwar, A. J. (**1992**). ''Theoretical and experimental study of a fiber optic microphone,'' J. Acoust. Soc. Am. **91**, 3049–3056.
Hubbard, A. (**1993**). ''A traveling-wave amplifier model of the cochlea,'' Science **259**, 68–71.
Johnstone, J. R., Alder, V. A., Johnstone, B. M., Roberstons, D., and Yates, G. K. (**1979**). ''Cochlear action potential threshold and single unit threshold,'' J. Acoust. Soc. Am. **65**, 254–257.
Khanna, S. M., and Leonard, D. G. B. (**1986**). ''Relationship between basilar membrane tuning and hair cell condition,'' Hearing Res. **23**, 55–70.
Kolston, P. J. (**1988**). ''Sharp mechanical tuning in a cochlear model without negative damping,'' J. Acoust. Soc. Am. **83**, 1481–1487.
Lighthill, J. (**1981**). ''Energy flow in the cochlea,'' J. Fluid Mech. **106**, 149–213.
Lynch, T. J., Nedzelnitsky, V., and Peake, W. T. (**1982**). ''Input impedance of the cochlea in cat,'' J. Acoust. Soc. Am. **72**, 108–123.
Müller, M. (**1996**). ''The cochlea place-frequency map of the adult and developing mongolian gerbil,'' Hearing Res. **94**, 148–156.
Nedzelnitsky, V. (**1980**). ''Sound pressures in the basal turn of the cat cochlea,'' J. Acoust. Soc. Am. **68**, 1676–1689.
Neely, S. T., and Kim, D. O. (**1986**). ''A model for active elements in cochlear biomechanics,'' J. Acoust. Soc. Am. **79**, 1472–1480.
Nuttall, A. L., and Dolan, D. F. (**1996**). ''Steady-state sinusoidal responses of the basilar membrane in guinea pig,'' J. Acoust. Soc. Am. **99**, 1556–1565.
Olson, E. S., and Borawala, S. (**1997**). ''The design and purpose of an intracochlear pressure sensor.'' in *Diversity in Auditory Mechanics*, edited by E. R. Lewis, G. R. Long, R. F. Lyon, P. M. Narins, C. R. Steele, and E. Hecht-Poinar (World Scientific, Singapore), pp. 347–353.
Olson, E. S., and Mountain, D. C. (**1991**). ''*In vivo* measurement of basilar membrane stiffness,'' J. Acoust. Soc. Am. **89**, 1262–1275.
Olson, E. S., and Mountain, D. C. (**1994**). ''Mapping the cochlea's mechanical properties to its cellular architecture,'' J. Acoust. Soc. Am. **95**, 395–400.
Peterson, L. C., and Bogart, B. P. (**1950**). ''A dynamical theory of the cochlea,'' J. Acoust. Soc. Am. **22**, 369–381.
Plassman, W., Peetz, W., and Schmidt, M. (**1987**). ''The cochlea in gerbilline rodents,'' Brain Behavior and Evolution **30**, 82–101.
Puria, S., and Allen, J. B. (**1991**). ''A parametric study of cochlear input impedance,'' J. Acoust. Soc. Am. **89**, 287–309.
Puria, S., and Allen, J. B. (**1997**). ''Cat middle-ear measurements and model: Evidence of acoustic delay in the tympanic membrane,'' Abstract 193 from the 20th Midwinter Research Meeting, Association for Research in Otolaryngology.
Puria, S., Peake, W. T., and Rosowski, J. J. (**1997**). ''Sound pressure measurements in the cochlear vestibule of human-cadaver ears,'' J. Acoust. Soc. Am. **101**.
Rhode, W. S. (**1971**). ''Observations of the vibration of the basilar membrane in squirrel monkeys using the Mossbauer technique,'' J. Acoust. Soc. Am. **49**, 1218–1231.
Ruggero, M. A., Rich, N. C., Robles, L., and Recio, A. (**1996**). ''The effects of acoustic trauma, other cochlear injury, and death on basilar-membrane responses to sound,'' in *Scientific Basis of Noise-Induced Hearing Loss*, edited by A. Axelsson *et al.* (Thieme Medical, New York), pp. 23–35.
Ruggero, M. A., Rich, N. C., Robles, L., and Shivalpuja, B. G. (**1990**). ''Middle-ear response in the chinchilla and its relationship to mechanics at the base of the cochlea,'' J. Acoust. Soc. Am. **87**, 1612–1629.
Ruggero, M. A., Rich, N. C., Recio, A., Srayan, S. S., and Robles, L. (**1997**). ''Basilar membrane responses to tones at the base of the chinchilla cochlea,'' J. Acoust. Soc. Am. **101**, 2151–2163.
Ryan, A. (**1976**). ''Hearing sensitivity of the mongolian gerbil, Meriones unguiculatus,'' J. Acoust. Soc. Am. **59**, 1222–1226.
Schloss, F., and Strasberg, M. (**1962**). ''Hydrophone calibration in a vibrating column of liquid,'' J. Acoust. Soc. Am. **34**, 958–960.
Sellick, P. M., Patuzzi, R., and Johnstone, B. M. (**1982**). ''Measurement of basilar membrane motion in the guinea pig using the Mossbauer technique,'' J. Acoust. Soc. Am. **72**, 131–141.
Steele, C. R. (**1974**). ''Behavior of the basilar membrane with pure-tone excitation,'' J. Acoust. Soc. Am. **55**, 148–162.
Steele, C. R., and Taber, L. A. (**1979**). ''Comparison of WKB calculations and experimental results for three-dimensional cochlear models,'' J. Acoust. Soc. Am. **65**, 1007–1018.
Taber, L. A., and Steele, C. R. (**1981**). ''Cochlear model including three-dimensional fluid and four modes of partition flexibility,'' J. Acoust. Soc. Am. **70**, 426–436.
Timoshenko, S. P., and Woinowsky-Krieger, S. (**1959**). *Theory of Plates and Shells* (McGraw–Hill, New York), Chap. 3.
Ulfendahl, M., and Khanna, S. M. (**1993**). ''Mechanical tuning characteristics of the hearing organ measured with the sensory cells in the gerbil temporal bone preparation,'' Pflugers Arch. Ges. Physiol. Menschen Tiere **424**, 95–104.
Xue, S., Mountain, D. C., and Hubbard, A. E. (**1995**). ''Electrically evoked basilar membrane motion,'' J. Acoust. Soc. Am. **97**, 3030–3041.
Zhou, G., Bintz, L., Anderson, D. Z., and Bright, K. E. (**1993**). ''A life-sized physical model of the human cochlea with optical holographic readout,'' J. Acoust. Soc. Am. **93**, 1516–1523.

Downloaded 30 Jun 2010 to 156.145.57.60. Redistribution subject to ASA license or copyright; see http://asadl.org/journals/doc/ASALIB-home/info/terms.jsp